INTERNATIONAL COUNCIL FOR EXPLORATION OF THE SEA

C.M. 1977/C:18

Hydrography Committee

LOW-FREQUENCY FLUXES OF MOMENTUM, HEAT, SALT AND NUTRIENTS AT THE EDGE OF THE SCOTIAN SHELF

by Peter C. Smith
Atlantic Oceanographic Laboratory
Bedford Institute of Oceanography
Dartmouth, N.S., Canada

ABSTRACT

Measurements of current, temperature, and salinity from a single mooring at the edge of the Scotian Shelf are analyzed for the period from December 1975 to April 1976. Major contributions to the subtidal Reynold's stresses consist of the wind-driven flows (2- to 8-day periods) and offshore forcing effects resembling topographic Rossby waves (10 to 30 days). These may be distinguished by a difference in sign of the onshore momentum flux in each band. Uniform divergence of these stresses across the shelf would not be significant to the general circulation. The

The shoreward eddy transport of salt and heat are maximum at 50 m depth and concentrated in the lowest frequency bands. Considered uniform at the open boundary, the 50-m fluxes would support temperature and salinity differences of 1.7°C and 0.6‰ along the Scotian Shelf.

Estimates of nutrient fluxes at the shelf break are made by establishing a relationship between nutrients and T/S properties through another variable, the concentration of dissolved oxygen. The subtidal shoreward transport of nitrate is found to be 12.4 μg at/m^2s, which nearly meets Fournier's (1977) estimate (15.5 μg at/m^2s) of the spring and summertime phytoplankton requirements on the shelf.

Finally, current meter and hydrographic data and satellite imagery are used to estimate the net salt and heat transports

produced by the entrainment of surface shelf water by a Gulf Stream eddy. On an annual basis (6 events/year), the contributions of salt and heat to the shelf waters are 3×10^{13} kg/yr and 6×10^{19} cal/yr, which are equivalent to the measured subtidal transports at the shelf break. These estimates exceed by a factor of 6 those of Voorhis et al. (1976) and Horne (1977) for small-scale frontal mixing.

INTRODUCTION

The low-frequency circulation near the edge of the Scotian Shelf has two important energy sources:

a. atmospheric variability caused by passing storms, and

b. fluctuating offshore currents such as the Gulf Stream.

The response of the Scotian Shelf waters to atmospheric events occurs primarily in two frequency ranges: the inertial band and at the dominant forcing frequencies. The inertial dynamics have been shown to conform to a variable depth mixed layer model (Smith et al., 1977). In the subtidal bands, the most energetic atmospheric forcing occurs at periods from 2.0 to 8.0 days as indicated by the wind stress and barometric pressure spectra in Figure 1. For the stormy winter period from December 1975 to April 1976, the main contribution to the variance of the pressure field is found near 4 days whereas the wind stress has important variability at 2- and 4-day periods. Although the amplitude of these spectra may change with season, the frequency range does not (Petrie and Smith, 1977). Analysis of current meter records from a 1967-1968 mooring program on the Scotian Shelf indicates that the dominant subtidal response in the water column is directly forced by the wind stress, that is, the growth and decay of peak currents and wind stresses closely correspond. Consequently, the current spectra

show wind-driven kinetic energy which is confined to a band from 2.5 to 7.0 day periods (Petrie and Smith, 1977).

The Gulf Stream system also provides an important mechanism for driving the circulation on the continental slope and rise at time scales somewhat longer than atmospheric. For periods of 8 to 20 days, Thompson (1971) and Thompson and Luyten (1976) have identified certain features of bottom-trapped topographic Rossby waves (Rhines, 1970) in current meter records from below the main thermocline on the continental rise south of New England. In addition to bottom intensification of the kinetic energy density, waves moving shoreward are characterized by a downslope flux of longshore (~ eastward) momentum. In a recent study, Luyten (1977) has traced this feature to the base of the rise at the 4000 m isobath, which suggests that these waves are forced by the Gulf Stream.

Above the thermocline, warm-core eddies shed by the Gulf Stream provide an important mechanism for mixing and exchange between the shelf and slope waters. Figure 2 is a satellite infrared image of sea surface temperature depicting such an eddy in the slope water south of Halifax on 27 March 1976. Cold surface shelf water is being entrained by the eddy in the two tongues along its eastern and western borders. The analysis of subsequent images indicates that the tongues wrapped around the eddy are ultimately incorporated into the slope water mass when the eddy is re-absorbed by the Gulf Stream. A similar event at the shelf break off New Jersey has been recently described by Morgan and Bishop (1977). From the current measurements to be reported here, it appears that the loss of surface shelf water is at least partially compensated by a deep return flow of slope water onto the Scotian Shelf. This replacement serves to inject large quantities of

salt and heat onto the shelf and also has important biological implications since the slope water is nutrient-rich.

Evidence that the slope water nutrients support enhanced biological activity over the outer portion of the shelf is given in recent measurements by Fournier et al. (1977), who found shelf-wide maxima in nutrient concentrations, biomass, and primary production there in all seasons. In this regime, nitrogen is the single most important nutrient since its concentration limits primary production on the shelf (Riley, 1967). Using a crude set of assumptions, Fournier estimated the nitrate supply rate necessary to support their measured production in the euphotic zone during the spring and summer months, April to September. If a continuous shoreward flux at the shelf break were the only source, then a net transport of 15.5 μg at/m^2s N in a 100-m water column is required. The important dynamical questions posed by this estimate are:

a. can the shelf break circulation provide nitrates to the shelf waters at this rate, and

b. if so, what are the dominant mechanisms involved?

In December 1975, scientists at Bedford Institute of Oceanography began a mooring experiment near the shelf break south of Halifax. The primary goals of this experiment were:

1. to define the low-frequency circulation,

2. to identify important exchange processes between the shelf and slope waters, and

3. to support biological studies on the shelf with estimates of nutrient fluxes at the shelf break.

The results presented here are derived primarily from a single pilot

mooring at the shelf break for the period from December 1975 to April 1976. In the third section these data will be analyzed to determine the low-frequency (subtidal) contributions to the shoreward fluxes of momentum, heat, salt, and nitrate. The first three quantities are computed directly from the cospectra of temperature, salinity and velocity, whereas the nutrient transport is calculated from the salt or heat flux using correlations between nitrate, dissolved oxygen, and salinity or temperature. To place the magnitudes of these transports in perspective, the equivalent salt and heat exchanges resulting from the interaction of a warm-core eddy with the shelf water are estimated in the fourth section. Then in the final section, these results are compared to recent estimates of heat and salt transport across the slope water boundary by smaller scale frontal processes (Voorhis et al., 1976; Horne, 1977).

THE SHELF BREAK EXPERIMENT

The mooring deployment for the shelf break experiment is illustrated in Figure 3. The full array, which was placed in July 1976, consists of 8 mooring sites (S1 to S8) and 11 separate moorings. Prior to the full deployment, a pilot mooring was placed at the S1 site (42°48'N, 63°30'W) near the shelf break where the nominal water depth is 250 m. The mooring carried instruments at depths of 50, 150, and 230 m and was supported by a subsurface float just above the 50-m instrument (actual depths varied slightly from these nominal levels). Aanderaa RCM-5 instruments were used to sample rate, direction, temperature, and conductivity at 20-minute intervals. Since the shelf break runs nearly east-west at S1, the currents were resolved to easterly (alongshore) and northerly (onshore) components (U, V) in the subsequent analysis and a time series of salinity was produced

from the temperature and conductivity records. The overall precision in current speed, direction, temperature, and salinity fluctuations is estimated at ±1.0 cm/s, ±3°, ±0.03°C, and ±0.1‰. The 20-minute sampling interval ensures that the spectral analyses of the records are not strongly aliased by internal waves, whereas the depth of the subsurface float kept the mooring well away from the surface wave action.

In conjunction with the mooring operations, extensive hydrographic measurements were made in the vicinity of the moorings. Primary emphasis was placed on three main sections along 63°25'W, 64°W and 43°N. These provide a three-dimensional view of the water mass distribution near the shelf break, as illustrated by the temperature and salinity fields in Figures 4a and 4b. In the upper 100 m, the 9° isotherm and the 34.5‰ isohaline mark the transition between coastal water at the surface and warm slope water defined by Gatien (1976). On this occasion (April, 1977) the slope water is seen to extend well onto the shelf whereas at other times its penetration is limited by a boundary of intense interleaving just off the shelf. A strong seasonal thermocline develops over the region in summer but the deep water mass properties (below 50 m) are relatively consistent throughout the year. The intense small-scale fluctuations of the isotherms and isohalines near the shelf break are largely caused by temporal variability associated with the internal tide (Petrie, 1975).

For the purpose of making the biologically relevant flux estimates, the dissolved oxygen content of shelf and slope waters was routinely measured with a Beckman monitor attached to the CTD. The O_2 profiles, contoured in Figure 4c, show high surface values which decrease monotonically with depth into the slope water down to the oxygen minimum at 200 to 300 m. In addition, on some cruises, discrete measurements of nutrients were taken from

rosette bottles on the CTD to complement the continuous O_2 data. Figure 4d shows the nitrate section along 63°25'W corresponding to the other sections in Figure 4. The increase of nitrate concentration with depth reveals the richness of the slope water mass and also confirms the well known inverse correlation between the concentrations of oxygen and nutrients. As with the other sections, most small scale vertical excursions of the contours near the shelf break are associated with temporal variability. On the other hand, the broad shoaling trend of the isopleths below 100 m between the slope and deep shelf water has been noted in other sections from different seasons and may be a more permanent feature of the shelf break circulation. In any case, it is clear that concentrated nitrates are present over the shelf from 50 m to the bottom where they become available for mixing and diffusion into the surface layers.

SUBTIDAL FLUXES OF MOMENTUM, HEAT, SALT, AND NUTRIENTS

The mean values of the current components, temperature, and salinity at the pilot mooring for the period from 13 December 1976 to 6 April 1977 are given in Table 1. The mean current vectors are nearly collinear and lie in the northeast quadrant at 50 m, 150 m, and the southwest quadrant at the bottom. The mean temperature and salinity levels are consistent with the hydrographic measurements in Figure 4.

Spectra of the 20-minute data were analyzed in blocks of 28.4 days using a fast Fourier transform technique. The shoreward components of eastward momentum, heat, and salt were then derived from the cospectra of the northward velocity fluctuations, V', with those of eastward velocity, U', temperature, T', and salinity, S'. Error bounds for the cospectral

quantities were estimated from the standard error of the mean using block statistics.

Momentum Fluxes. The kinetic energy spectra showing the major contributions to the variance in the current field at S1 are presented in Figure 5. The tidal and inertial peaks are familiar features in this regime representing roughly 50% of the current variance in this winter season. In the subtidal range, the responses to atmospheric events at 2-to 8-day periods and deep-ocean forcing at 8 to 30 days account for 40% of the variance in winter, dropping to 20% in summer due to a reduction in the level of atmospheric forcing.

One characteristic of topographic Rossby waves which has been observed by Thompson and Luyten (1976) on the continental rise is the tendency toward bottom-trapping in the structure of kinetic energy density at the highest frequencies (shortest wavelengths). Given the stratification and depth range at S1, this structure would be essentially barotropic at the smallest typical wavelengths (50 to 100 km). A trend toward vertical uniformity is evident in the first three spectral estimates at 150 and 230 m but it is probably not significant.

Another more definite feature of topographic waves is found in Figure 6. A negative (downslope) flux of eastward momentum is revealed by the co-spectrum of U' and V' in a low-frequency band centered at 14 days. On the other hand, the momentum flux in the wind-driven bands is positive and produces a distinct separation of the two phenomena. This difference of sign is maintained by counterclockwise axis rotations up to 30°, which represents the ambiguity between onshore directions measured relative to the coastline and to the shelf break. Unfortunately, because of poor statistical confidence in all the spectral estimates, the connection

between the low-frequency current measurements and topographic Rossby waves is very tenuous. Furthermore, the fortuitous separation of the two low-frequency processes in the U'·V' cospectrum is interesting but reveals very little about subtidal dynamics. However some useful comparisons are provided by estimates of the magnitude of the onshore momentum fluxes in the context of a very simple model for the mean flow.

The average currents in Table 1 suggest that the mean flow U at S1 is roughly parallel to the coast at 5 to 10 cm/s, whereas the nearshore flow is estimated to be of order 10 cm/s in the opposite direction (Sutcliffe et al., 1976). In simple equilibrium this flow may be balanced by mean wind stress, surface pressure gradients, bottom stress, and the divergence of Reynold's stresses. The vertically-averaged momentum equations are then given by

$$0 = -(\overline{U'V'})_y - g\eta_x + \frac{\tau_w^x - \tau_b^x}{\rho h} \tag{1}$$

$$0 = -fU - g\eta_y - (\overline{V'^2})_y \tag{2}$$

The mean wind stress over the mooring period was 0.43 dyne/cm^2 and the bottom stress may be estimated from the magnitude of the mean alongshore current, U(≈10 cm/s), according to a linearized formula of Rooth (1972),

$$\tau_b^x = \frac{3\rho}{2} C_D \bar{C} U$$

where $C_D = 2.0 \times 10^{-3}$ and $\bar{C}$(≈20 cm/s) is the rms amplitude of the current fluctuations. An upper limit on the magnitude of the alongshore surface

slope, η_x, may be estimated at -1.4×10^{-7} from measurements by Scott and Csanady (1976) off Long Island. Then assuming the Sl Reynold's stresses diverge uniformly across the shelf (width $\sim$ 100 km, depth h $\sim$ 100 m), the estimates given in Table 2 are obtained for the terms in Equations 1 and 2. Note that under these assumptions, an onshore surface slope, $-\eta_y$, of order 10^{-6} must be invoked for balance. It is also clear from these calculations that the divergence of the shelf break momentum fluxes is insignificant compared to the other forces acting on the shelf waters.

Heat and Salt Fluxes. Unlike the kinetic energy, the variability in temperature and salinity fields is concentrated at the lowest frequencies. The temperature spectra plotted in Figure 7 show that this is particularly true at the 50-m level where the variance at periods greater than 7 days represents 55% of the total variance and exceeds that in both the wind-driven (16%) and tidal (18%) bands. At 150 m, the contribution at the lowest frequencies drops to 48% and at 230 m it is 35%. Furthermore, temperature and salinity fluctuations are highly correlated at subtidal frequencies (coherences exceed 0.95 in the most energetic bands) so the same spectral distribution of variance is found in the salinity field.

The cospectrum of northward velocity and temperature $V' \cdot T'$ in Figure 8(a) reveals a strong onshore heat flux at 50 m in the subtidal range. The largest contributions to this flux occur at the lowest frequencies but there are distinct contributions in the wind-driven bands. At 150 m there is much weaker onshore flux in which the low frequencies are no longer dominant, and at 230 m the subtidal heat flux is offshore. Although the statistical significance of the net flux at the two deeper levels is questionable, the onshore component at 50 m is clearly positive. A similar

spectral distribution is found for the subtidal salt flux in Figure 8(b). The 50-m flux is again definitely onshore and in this case there is also a significant onshore salt flux at 150 m in the wind-driven band (coherence level of 0.76 at 4-day periods).

The reason for the intense variability at 50 m relative to that at 150 and 230 m may be seen in the hydrographic sections in Figure 4. At the shelf break, a strong front between the coastal and slope water lies near the 50-m sensor where the average temperature, for instance, is near 6°C but the extreme temperatures are 2° and 12°C. In contrast, the mean temperature at 150 m is near 11° and the extrema are 10° and 12°C. The cospectral results at 50 m signify that on average the 2° water is moving offshore and the 12° water moving onshore. If the subtidal salt and heat fluxes at 50 m were distributed over the upper 100 m of the water column and the alongshore transport of shelf water taken to be 10 cm/s (see Sutcliffe et al., 1976), then the low-frequency fluxes alone could support temperature and salinity differences of roughly 1.7°C and 0.6‰ along the Scotian Shelf. The consistency of these estimates with measured longshore gradients on the shelf will be examined in a separate paper (Houghton et al., 1977).

Nutrient fluxes. Since the subtidal fluxes of heat and salt represent a low-frequency diffusion of slope water properties into the coastal water, a similar estimate for nitrate diffusion may be made using the measured transports and a local correlation between nitrates and T/S properties. Naturally, this assumption implies that the dominant time scales for the shoreward flux of nitrogen are the same as those for heat and salt, i.e. periods greater than 10 days. If valid, this result may have important consequences with regard to the timing and duration of the spring bloom on the shelf.

For practical reasons, the method used to estimate the shoreward nitrate flux is somewhat indirect. Sparsely sampled nutrient data, such as those represented in Figure 4(d), taken in the vicinity of the shelf break demonstrate that a strong inverse correlation exists between nitrate and dissolved oxygen concentrations at least for depths of 50 m to 300 m. Figure 9 illustrates the quality of this correlation for stations along 63°30'W in July 1976. However, covariances between physical (T,S) and biological parameters (NO_3, PO_4, O_2) were found to be quite variable over the broad survey area so that stable relationships between the two could only be defined locally, i.e. in the vicinity of the mooring at sensor depth. Since much more oxygen data (discrete samples as well as continuous profile data) than nutrients were regularly gathered, the most significant local correlations were produced between the oxygen O_2 and temperature T or salinity S variables. Figure 10(a) shows the excellent correlation between discrete samples of oxygen and salinity from a depth of 50 m on 63°30'W for the July 1976 cruise. Superimposed on these data is a summary of the digitized profile data from the same cruise for which each point represents a 10-m average of all the O_2 values found in a 0.5‰ salinity interval. The digit next to each point indicates the number of values over which each sample was taken. The total number of continuous data points (1453) contributing to the 10-m average confirms the significance of the 50-m correlation over this range. The seasonal stability of this relationship in the shelf break region is illustrated in Figure 10(b) where it is compared to the results for data from two different cruises in December 1975 and October 1976. The December correlation, representing discrete sample data at 50 m on 63°30'W, shows generally higher oxygen levels but with the same trend as the July data. The October curves, on the other hand, are derived

from 10-m averages of the profile data along 63°30'W, but they too show roughly the same slope. In a similar manner, localized relationships were developed between temperature and oxygen variables at 50 m and also at the other sensing depths (150, 230 m). Although the correlations with salinity were generally tighter than with temperature, each gave a negative regression at 50 m, positive at 150 m, and nearly zero at 230 m as indicated in Table 3.

Once the relationships between nitrates, oxygen and salinity (temperature) are established, the subtidal nitrate transport may be computed by multiplying the corresponding salt (heat) flux by the product of the NO_3 vs. O_2 and O_2 vs. S(T) regressions. Since T and S are highly correlated in this region, the nitrate flux estimates derived from the salt and heat fluxes at a given depth should be consistent and their difference indicates some of the uncertainty in the calculation. The results at all three depths are given in Table 3. The shoreward nitrate transports are maximum at 50 m, negative at 150 m, and vanishing at 230 m. As expected, the strong heat and salt fluxes at the shallowest level imply an onshore diffusion of nutrients whose magnitude exceeds those at the deeper levels by a factor of 3 or 4. On the other hand, the positive slopes of the 150 m correlations transform the weak onshore salt and heat fluxes (Figure 8) into an offshore nitrate flux. This effect may be due to the competing influence of a mean upwelling at the shelf break which maintains a negative onshore oxygen gradient by drawing up oxygen-poor water along the bottom [e.g. Figure 4(c), (d)]. Finally, the vanishing gradients at 230 m result because the sensing depth coincides with that of the oxygen minimum layer where the oxygen concentration is locally uniform.

For comparison with the nitrate requirements on the shelf (Fournier et al., 1977), the 50 m and 150 m were averaged to give the shoreward transport over that 100-m range. The resulting combined estimate of 12.4 μg at/m^2s from both salt and heat fluxes is certainly of the right order to meet the demand (15.5 μg at/m^2s). Thus the subtidal diffusion of nitrates across the shelf break in winter is sufficient to provide the shelf-wide productivity requirement of this crucial nutrient in spring and summer.

LARGE SCALE INTERACTIONS BETWEEN SHELF WATER AND WARM-CORE EDDIES IN THE SLOPE WATER

Between 60° and 65°W off the Scotian Shelf, the Gulf Stream regularly sheds anticyclonic warm-core eddies into the slope water. These features are typically 100 km in scale and generally drift westward along the continental slope and rise until they dissipate or are re-absorbed by the Stream. Frequently the eddies impinge on the continental shelf, interact with the shelf water through entrainment as illustrated by the satellite image in Figure 2. A similar event in the Mid-Atlantic Bight has been documented by Morgan and Bishop (1977) who concluded that the exchange process in the horizontal plane, i.e. compensating onshore flows occurred barotropically on either side of the offshore tongue of shelf water. Based on a total of three 90-day events, they estimated the annual volumetric exchange between shelf and slope waters of 208 km^3/yr.

Although the factors which control the growth and movement of eddies are not known, it is often possible to trace their development by analyzing a sequence of satellite infrared images. For example, the life history for the eddy shown in Figure 2 is depicted by the series of NOAA-4 VHRR analyses

in Figure 11. The eddy was formed from the large meander located between 62° and 64°W at 40°N on 16-18 February 1976. Notice the presence of an adjacent eddy at 67°W, which has already begun to entrain shelf water. By the end of February [Figure 11(b)], the eastern eddy had been shed but the western one had been re-absorbed into a large meander of the stream at 67°W. The analysis for 27-29 March [Figure 11(d)] is based on data shown in Figure 2. It shows the eddy in the process of entraining two different protrusions of shelf water. The eastern tongue which stretches southward to nearly 38°N is caused by the eddy's own anticyclonic circulation whereas the presence of the western tongue is the result of the continuing influence of the large meander at 67°W. Finally, in the last two frames [(e) and (f)], there is evidence for the re-absorption of the second eddy by the Gulf Stream. By mid-April the slope water regime has been re-established north of 40°N and the eddy has vanished along with its entrained quantities of shelf water.

Although there are no direct measurements to confirm the details of the eddy interaction event, certain aspects of the current meter records from the shelf break mooring suggest that important transfers of salt and heat were occurring while the eddy was actively entraining shelf water. Figure 12(a) shows vector plots for the filtered 6-hour currents at 50 m and 150 m for the period from 14 February to 14 April, 1976. For this period, the average onshore components at both 50 m (0.51 cm/s) and 150 m (1.44 cm/s) are weak, but strong low-frequency oscillations are evident in the records. In particular, there is a strong southwesterly pulse at 50 m during the first week in March (when the eddy to the south has begun to entrain shelf water) followed by a relaxation toward the middle of the month. During the period of strongest offshore flow at 50 m, the net onshore component at 150 m is weak but positive suggesting an exchange

in the vertical as well as the horizontal plane. Although there were several atmospheric events during this period, including a major storm around 17 March, their durations were consistently limited to two or three days.

The perturbation heat and salt flux vectors, computed as deviations from the mean values in Table 1, are plotted in Figures 12(b) and (c). These data reveal strong northward transports associated with the early March event, particularly at 50 m, and again at the end of the month at 150 m. The average onshore flux within each major pulse is more than four times the record mean. Furthermore, the mean shoreward components for both fluxes at each level are positive for the period shown. Once again it is important to emphasize that there are no unusual atmospheric events directly associated with either of the northward pulses.

In order to assess the importance of the eddy entrainment mechanism to the overall mixing processes between coastal and offshore waters, an attempt was made to estimate the net exchanges of salt and heat involved in this particular event. The most difficult quantity to determine is the volume of shelf water which is ultimately captured when the eddy is re-absorbed. This estimate was obtained by measuring the surface area ($\sim 5 \times 10^4$ km^2) of the crosshatched region in Figure 13(a) and then multiplying by an average depth ($\sim$50 m) of the shelf water layer indicated by the profile data in Figure 13(b). The volume of entrained shelf water thereby calculated is 2500 km^3 and is probably only accurate to within a factor of 2. The associated exchanges salt and heat may then be computed, be calculated by assuming a compensating return flow of slope water to the shelf and utilizing gross temperature, ΔT, and salinity, ΔS, differences beteeen the two water masses from Figure 13(b) (e.g. between 20 and 150 m). Notice that this

assumption implies that the circulation occurs in the vertical plane; however, the results are not changed substantially if a horizontal exchange with the slope water is assumed. With $\Delta T = 5°C$ and $\Delta S = 2.5‰$, the eddy interaction event is equivalent to total transports of 6.3×10^{12} kg of salt and 1.3×10^{19} cal of heat into the shelf water.

A degree of confidence in these results is produced by the analysis of a strikingly similar event which occurred in April/May 1977. The structure of the shelf and slope water masses prior to this event is illustrated in Figure 4 and the net volumetric, salt and heat exchanges were 1500 km^3, 3.8×10^{12} kg salt, and 9×10^{18} cal heat.

DISCUSSION

An examination of measured subtidal transports at the edge of the Scotian Shelf during the winter of 1975-1976 has shown that the magnitude of momentum flux is insignificant to the mean circulation on the shelf. However, the shoreward transports of salt, heat, and nutrients at the lowest frequencies (10 to 30 day periods) make significant contributions to the overall budgets for these quantities in the shelf waters. In particular, the subtidal flux of nitrates is capable of supporting measured primary production on the shelf in spring and summer.

From another point of view, two recent investigations at the slope water boundary by Voorhis et al. (1976) off New England and Horne (1977) near the Laurentian Fan have produced estimates of the net salt and heat fluxes into the shelf water due to small scale mixing processes such as double diffusion. These two quite similar results are compared to the present subtidal estimates at the shelf break in Table 4. On an annual basis, the subtidal fluxes are at least a factor of 6 greater than those associated with the frontal processes.

A further comparison is provided by computing the influence of the eddy-entrainment mechanism on the annual shelf/slope water exchange. An examination of three years worth of satellite imagery reveals that the entrainment events occur between 60° and 70°W at a rate of 6 per year (18 identifiable events during 1974-1976). Projection of the average transports involved in the March 1976 and April/May 1977 interactions to an annual basis gives results which are quite consistent with the measured subtidal fluxes (Table 4). The heat transports alone represent close to 30% of the annual solar input to the shelf (1.9×10^{20} cal/yr, see Horne, 1977), as compared to the 5% produced by frontal mixing. Thus, although the small scale processes are important for boundary mixing and dissipation within each water mass, the primary exchange between shelf and slope waters occurs via large scale, low frequency events.

Acknowledgements. The author would like to thank his friend and colleague, Dr. Brian Petrie, for his collaboration in the mooring program and many useful discussions of the data. Thanks are also due to many members of the Coastal Oceanography Division for their support in gathering, analyzing, and presenting the data. In addition, the kind cooperation of Dr. S. Peteherych of the Atmospheric Environment Service, Downsview, Ontario, in providing satellite imagery is appreciated.

REFERENCES

Fournier, R.O., J. Marra, R. Bohrer, and M. Van Det, Plankton dynamics and nutrient enrichment of the Scotian Shelf. Journal of the Fisheries Research Board of Canada, 34, 1004-1018, 1977.

Gatien, M.G., A study in the slope water region south of Halifax, Journal of the Fisheries Research Board of Canada, 33, 2213-2217, 1976.

Gill, A.E., and A.J. Clarke, Wind-induced upwelling, coastal currents and sea-level changes, Deep-Sea Research, 21, 325-345, 1974.

Horne, E.P.W., Interleaving at the subsurface front in the slope water off Nova Scotia, submitted to Journal of Geophysical Research.

Houghton, R.W., P.C. Smith and R.O. Fournier, in preparation, 1977.

Luyten, J.R., Scales of motion in the deep Gulf Stream and across the Continental Rise, Journal of Marine Research, 35,, 49-73, 1977.

Morgan, C.W., and J.M. Bishop, An example of Gulf Stream Eddy-induced water exchange in the Mid-Atlantic Bight, Journal of Physical Oceanography, 7, 472-479, 1977.

Munk, W.H., F.E. Snodgrass, and M.J. Tucker, Spectra of low-frequency ocean waves, Bulletin of Scripps Institution of Oceanography, 7, 283-362, 1959.

Petrie, B., M2 surface and internal tides on the Scotian Shelf and Slope, Journal of Marine Research, 33, 303-323, 1975.

Petrie, B., and P.C. Smith, Low-frequency motions on the Scotian Shelf and Slope, accepted for publication in Atmosphere, 15 (3), 1977.

Rhines, P.B., Edge-, bottom-, and Rossby Waves in a rotating, stratified fluid, Geophysical Fluid Dynamics, 1, 273-302, 1970.

Riley, G.A., Mathematical model of nutrient conditions in coastal waters, Bulletin of the Bingham Oceanographic Collection, 19, 72-80, 1967.

Smith, P.C., B. Petrie, and C.R. Mann, Circulation, variability and dynamics of the Scotian Shelf and Slope, submitted to Journal of the Fisheries Research Board of Canada, March 1977.

Thompson, R., Topographic Rossby waves at a site north of the Gulf Stream, Deep-Sea Research, 18, 1-19, 1971.

Thompson, R., and J.R. Luyten, Evidence for bottom-trapped Rossby waves from single moorings, Deep-Sea Research, 23, 629-635, 1976.

Voorhis, A.D., D.C. Webb, and R.C. Millard, Current structure and mixing at the shelf/slope water from south of New England, Journal of Geophysical Research, 81, 3695-3708, 1976.

TABLE 1. Mean conditions at mooring S1

December 1975 to April 1976

Nominal Depth	$\bar{U}$(east) (cm/s)	$\bar{V}$ (north) (cm/s)	$\bar{T}$ (°C)	$\bar{S}$ (‰)
50 m	8.52	2.81	6.09	33.38
150 m	4.75	2.56	10.79	35.46
230 m	-2.76	-0.87	9.71	35.47

TABLE 2. Magnitude of terms in mean momentum equations

($f = 10^{-4}/s$)

(1) Alongshore		(2) Onshore	
Term	Magnitude ($\times 10^5$ cm/s^2)	Term	Magnitude ($\times 10^5$ cm/s^2)
$-(\overline{U'V'})_y$	0.1	$-(\overline{V'^2})_y$	0.3
$\tau_w{}^x/\rho h$	4.3	$-fU$	100
$-\tau_b{}^x/\rho h$	6.0	$-g\eta_y$	?
$-g\eta_x$	+14.4		

TABLE 3. Shoreward subtidal nitrogen fluxes, $\overline{V'N'}$, at Mooring S1

December 1975 to April 1976

Nominal Sensing Depth	$(\partial O_2'/\partial T')$ (ml/l/°C)	$(\partial O_2'/\partial S')$ (ml/l/‰)	$(\overline{V'N'})_T$ (μg at/m²s)	$(\overline{V'N'})_S$ (μg at/m²s)
50 m	-0.127	-0.538	27.6	39.7
150 m	0.450	0.636	-8.63	-8.67
230 m	∿0	∿0	∿0	∿0

NOTE: The slope of the NO_3 vs. O_2 regression from Figure 9 is given by

$$\left(\frac{\partial N'}{\partial O_2'}\right) = -5.05 \text{ (μg at/l)/(ml/l)}$$

Then the nutrient fluxes are computed from the formulae

$$\overline{V'N'} = \left(\frac{\partial N'}{\partial O_2'}\right)\left(\frac{\partial O_2'}{T'}\right)\overline{V'T'} \text{ or } \left(\frac{\partial N'}{\partial O_2'}\right)\left(\frac{\partial O_2'}{\partial S'}\right)\overline{V'S'}$$

TABLE 4. Annual salt and heat exchange between shelf and slope water

Mechanism	Salt Transport ($\times 10^{-13}$ kg/yr)	Heat Transport ($\times 10^{-19}$ cal/yr)	% Annual Solar Input
Measured subtidal flux:	3.0	6.5	33
Large-scale eddy interaction:	3.0	6.0	30
Small-scale frontal processes			
Voorhis et al. (1976)	0.50	0.98	5
Horne (1977)	0.14	0.90	5

FIGURE CAPTIONS

Figure No.

1. Wind stress and barometric pressure spectra at Sable Island for period December 1975 to April 1976. Error bars are 95% confidence limits (Munk et al., 1959).

2. NOAA-4 infrared image of sea surface temperature on 27 March 1976 showing interaction between warm-core Gulf Stream eddy and surface shelf water.

3. Summary of Shelf Break Mooring Program. Present data taken from mooring S1 at the shelf break.

4. Hydrographic sections in the vicinity of the moorings in April 1977:
   (a) temperature
   (b) salinity
   (c) dissolved oxygen concentration
   (d) nitrate concentration

5. Spectra of kinetic energy at the shelf break mooring, S1, for December 1975 to April 1976. Error bars are the 95% confidence limits (Munk et al., 1959).

6. Low-frequency shoreward momentum flux at the shelf break mooring, S1, for December 1975 to April 1976. Error bars represent standard error of the mean based on block statistics.

7. Temperature spectra at the shelf break mooring, S1, for December 1975 to April 1976. Error bars are the 95% confidence limits (Munk et al., 1959).

8. (a) Low-frequency shoreward heat flux at S1, December 1975 to April 1976.
   (b) Low-frequency shoreward salt flux at S1, December 1975 to April 1976.

Error bars represent standard error of the mean based on block statistics.

9. Correlation between nitrate and dissolved oxygen concentrations for depths greater than 50 m on 63°30'W, 42° to 43°N, in July 1976.

10. Dissolved oxygen vs. salinity at 50 m on 63°30'W, 42° to 43°N.

    (a) Comparison of correlation of bottle samples with digitized data from oxygen monitor. Each symbol for digitized data represents average O_2 value over 0.5‰ salinity range. Numbers denote samples in that range.

    (b) Comparison of bottle and digitized data from three different cruises: December 1975; July 1976; October 1976.

11. 'Experimental Gulf Stream Analysis' from NOAA-4 infrared imagery, February to April 1976. Analysis performed by Environmental Products Group, NOAA-NESS, Washington, D.C.

12. Filtered vector plots from shelf break mooring.

    (a) 6-hour currents (U, V)

    (b) eddy heat flux ($\overline{U'T'}$ $\overline{V'T'}$)

    (c) eddy salt flux ($\overline{U'S'}$, $\overline{V'S'}$)

    Cartwright filter with low pass cutoff at 0.75 cpd effectively removes energy at frequencies of 1.0 cpd and greater.

13. Analysis of eddy interaction event on 27 March 1976:

    (a) surface area of entrained shelf water

    (b) temperature and salinity profiles from selected CTD stations

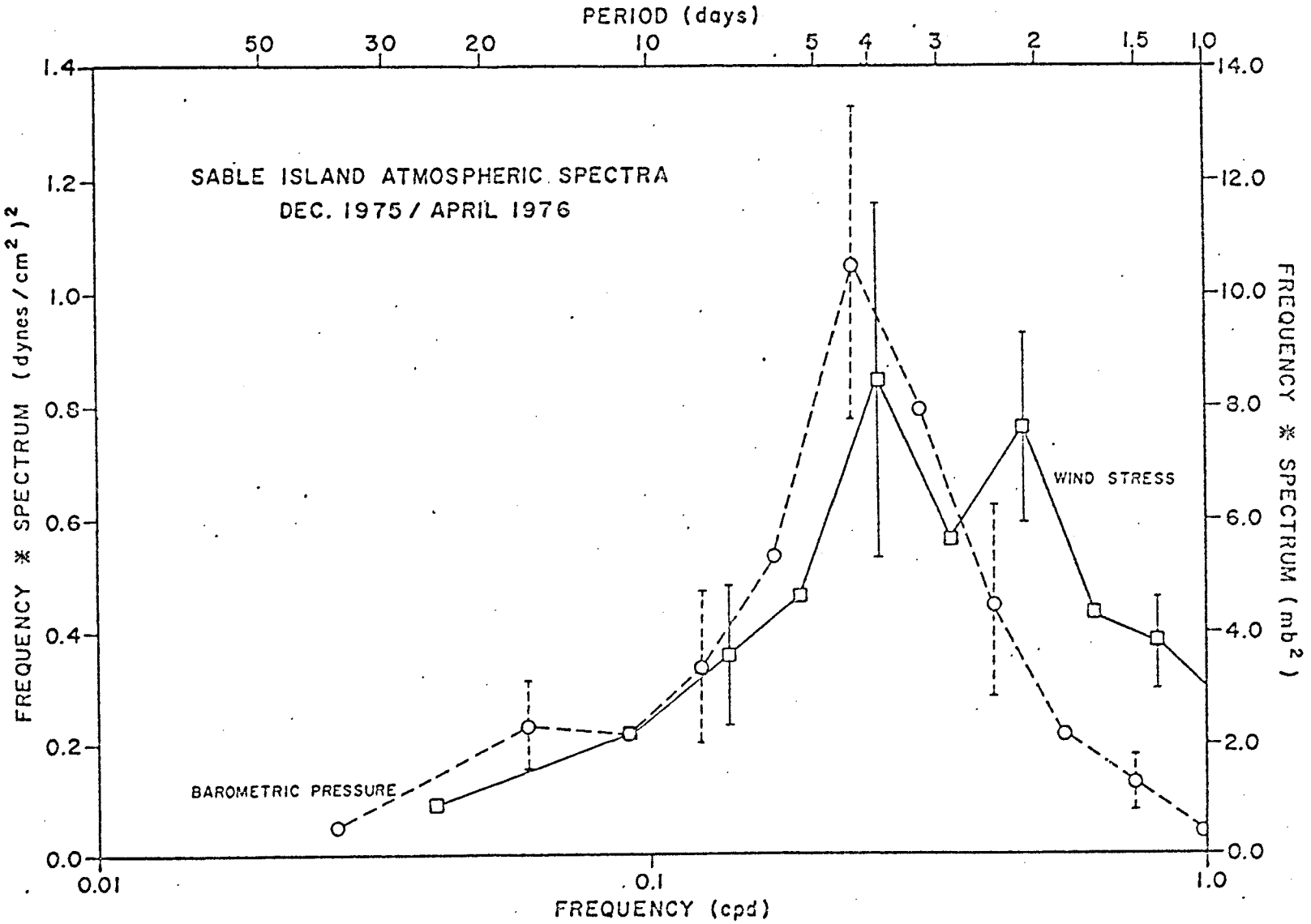
PERIOD (days)
50
30
20
10
5
4
3
2
1.5
1.0
SABLE ISLAND ATMOSPHERIC SPECTRA
DEC. 1975 / APRIL 1976
FREQUENCY * SPECTRUM (dynes / cm²)²
FREQUENCY * SPECTRUM (mb²)
1.4
1.2
1.0
0.8
0.6
0.4
0.2
0.0
14.0
12.0
10.0
8.0
6.0
4.0
2.0
0.0
WIND STRESS
BAROMETRIC PRESSURE
0.01
0.1
1.0
FREQUENCY (cpd)

Fig 1

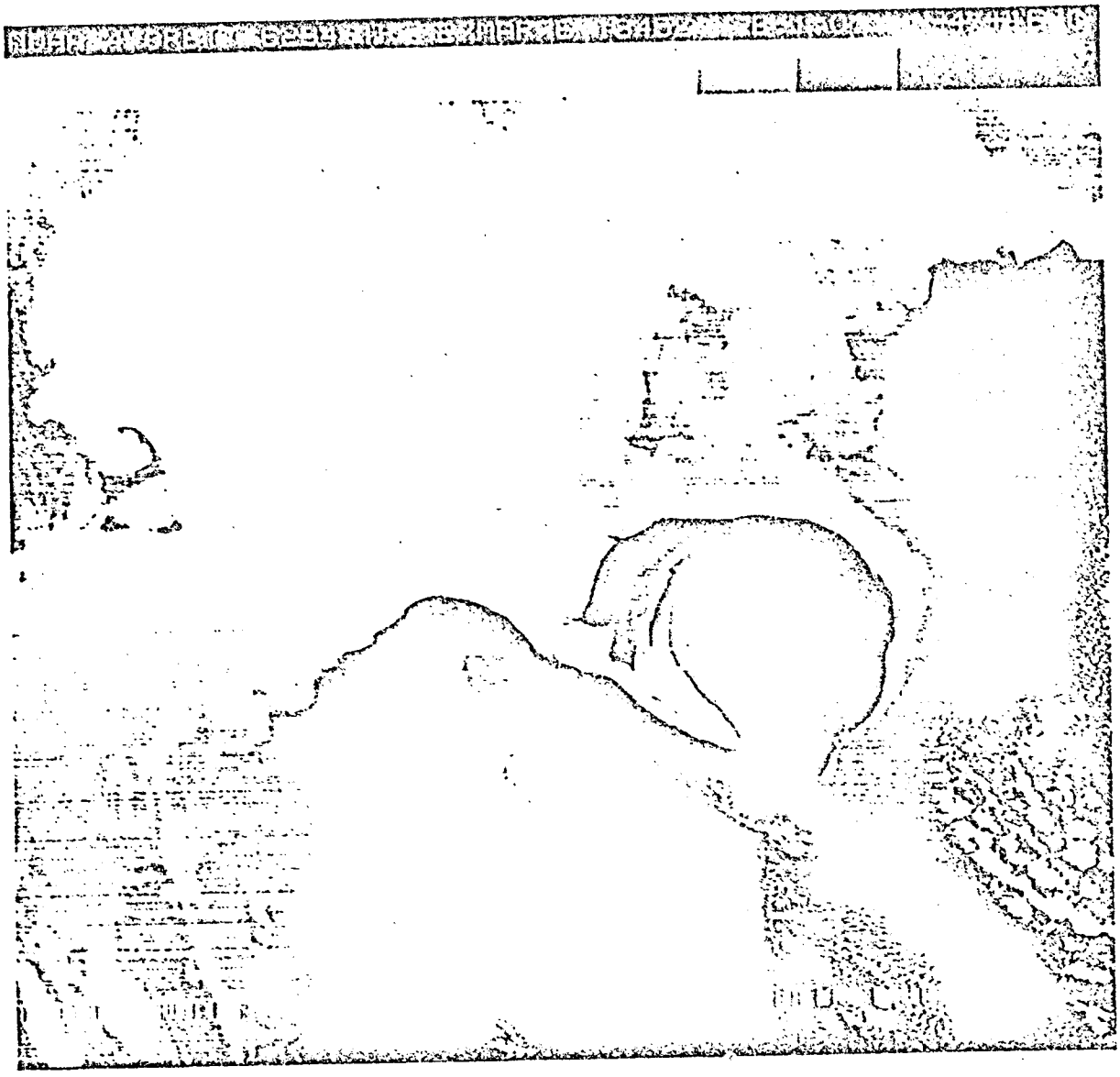

FIG 2

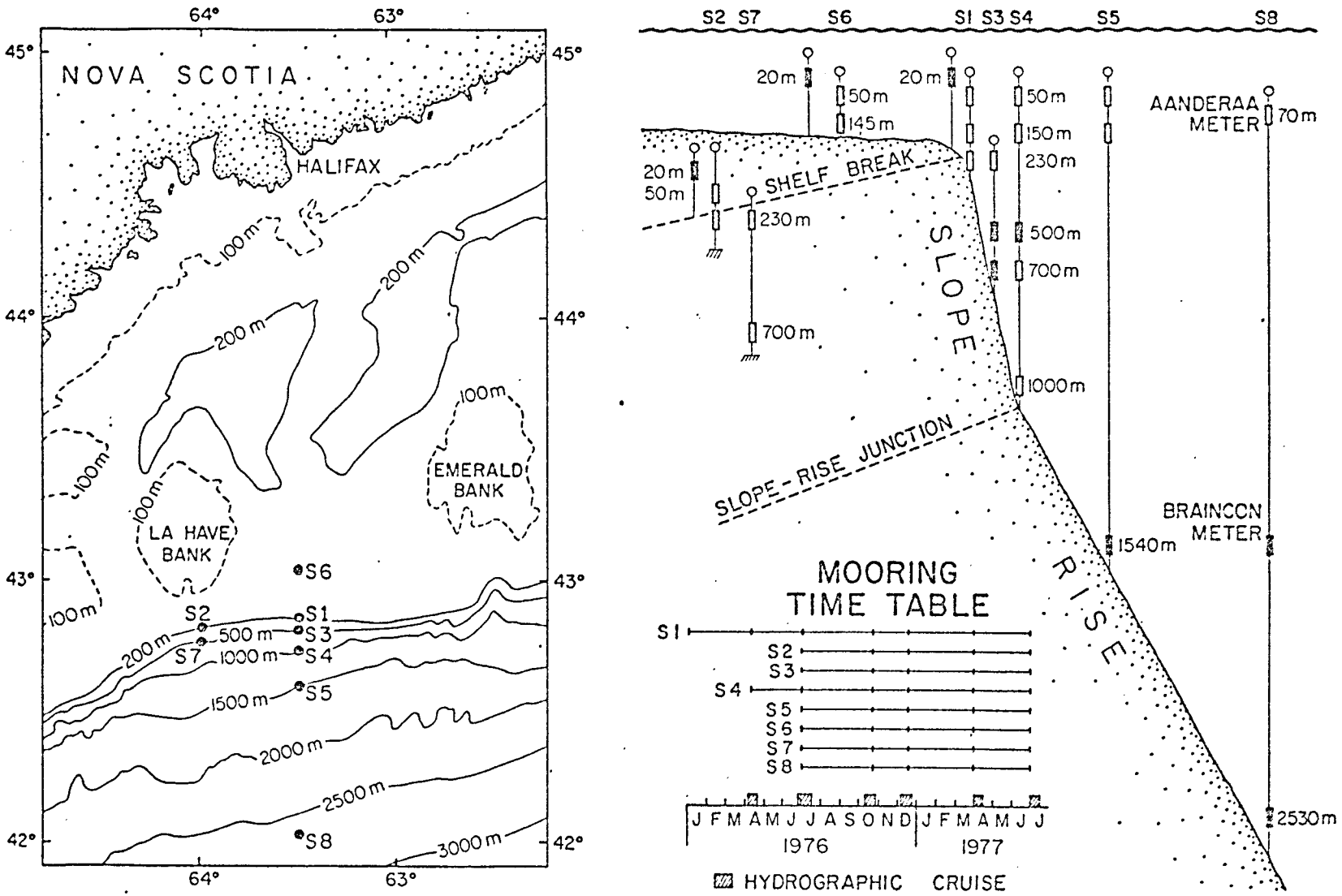
64°
63°
45°
44°
43°
42°
NOVA SCOTIA
HALIFAX
100m
200m
EMERALD BANK
LA HAVE BANK
S1
S2
S3
S4
S5
S6
S7
S8
500 m
1000 m
1500 m
2000 m
2500 m
3000 m
S2 S7
S6
S1 S3 S4
S5
S8
20m
50m
145m
150m
230m
500m
700m
1000m
1540m
2530m
SHELF BREAK
SLOPE
SLOPE-RISE JUNCTION
RISE
AANDERAA METER
BRAINCON METER
MOORING TIME TABLE
J F M A M J J A S O N D J F M A M J J
1976
1977
HYDROGRAPHIC CRUISE

FIG 3

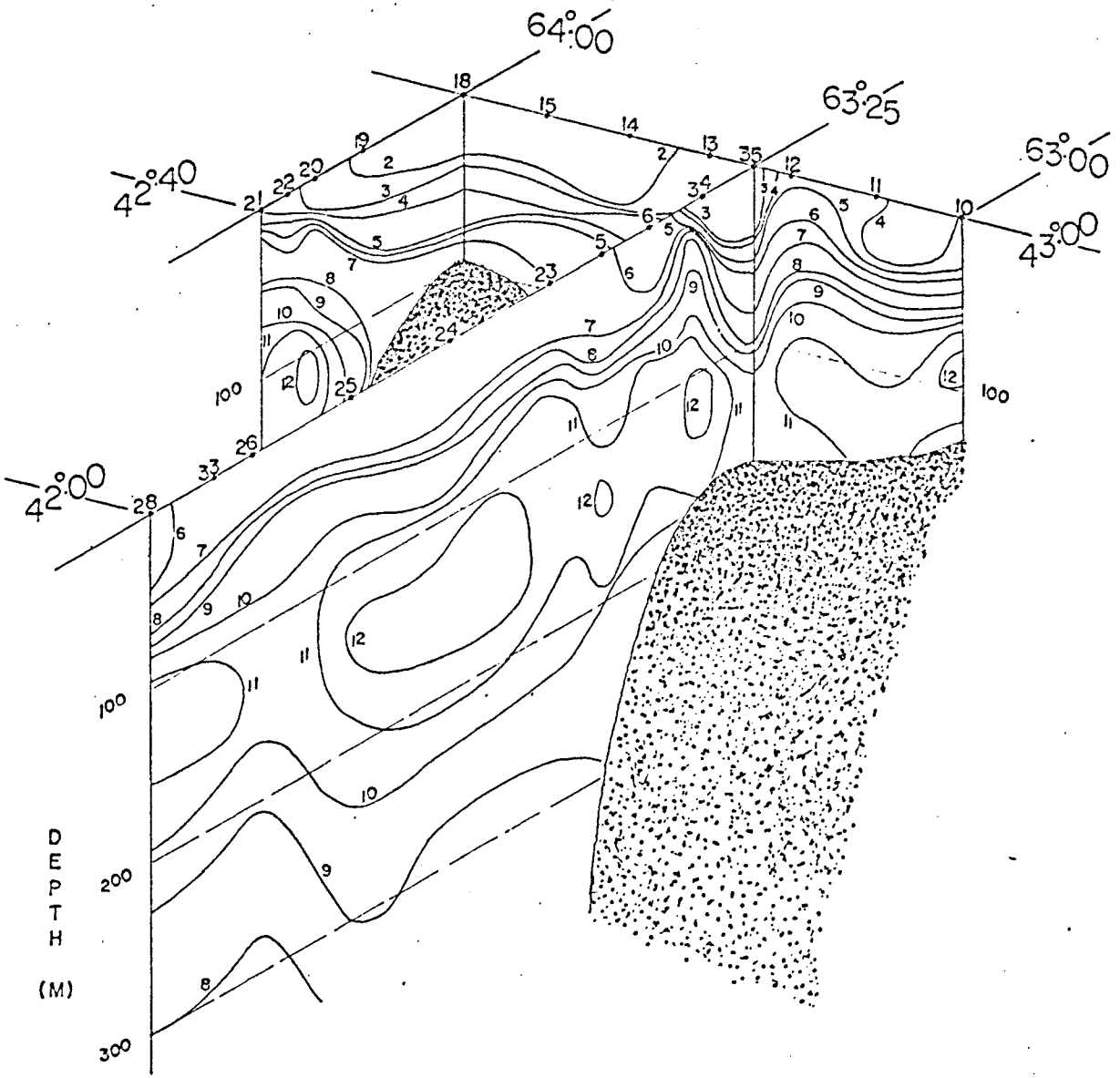

FIG 4(a)

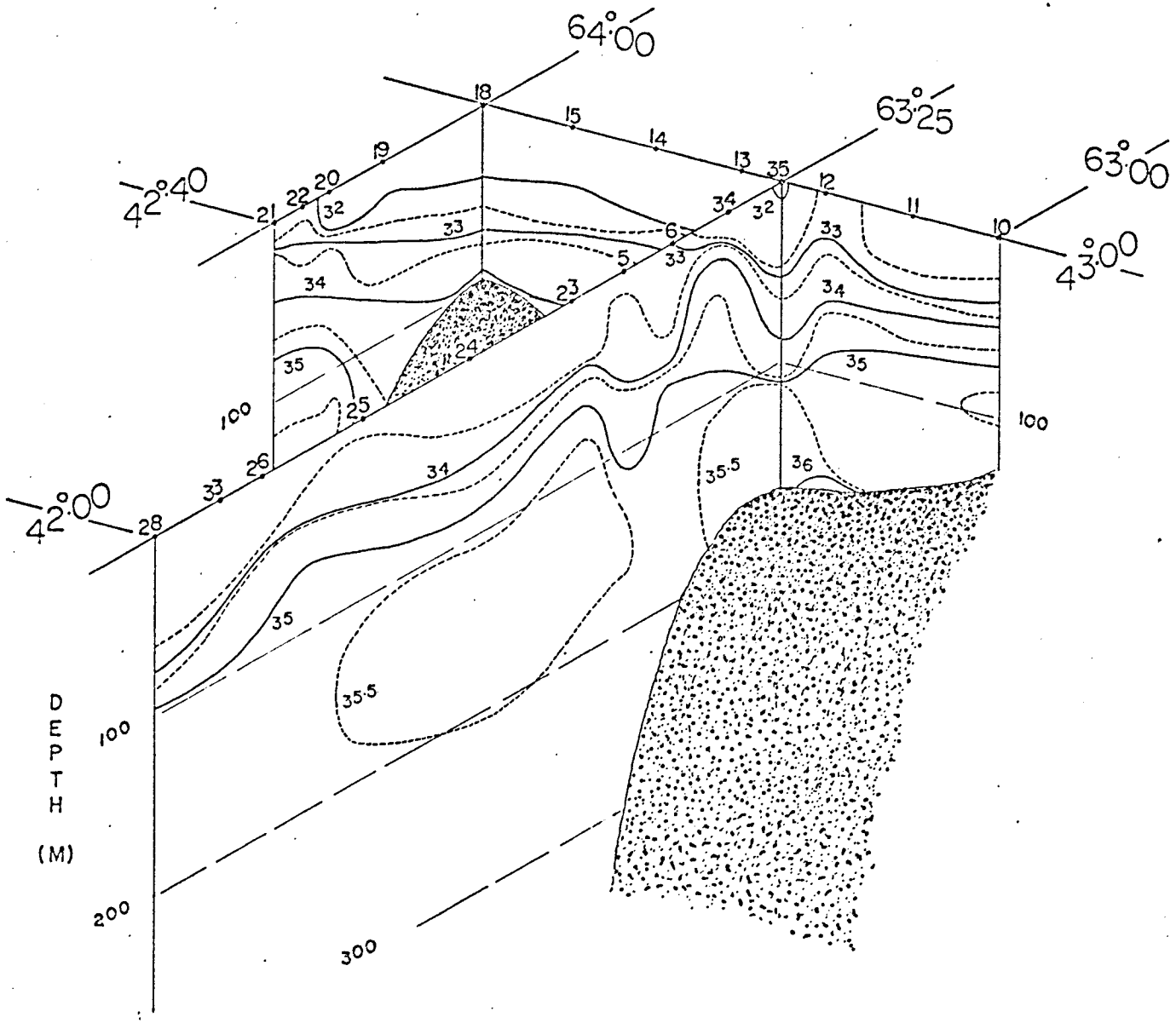
64°00
63°25
63°00
42°40
43°00
42°00
18
15
14
13
35
12
11
10
19
20
22
21
32
33
34
32
33
6
5
33
34
23
24
35
25
100
26
33
28
34
35
35.5
36
35
100
35.5
DEPTH (M)
100
200
300

FIG 4 (b)

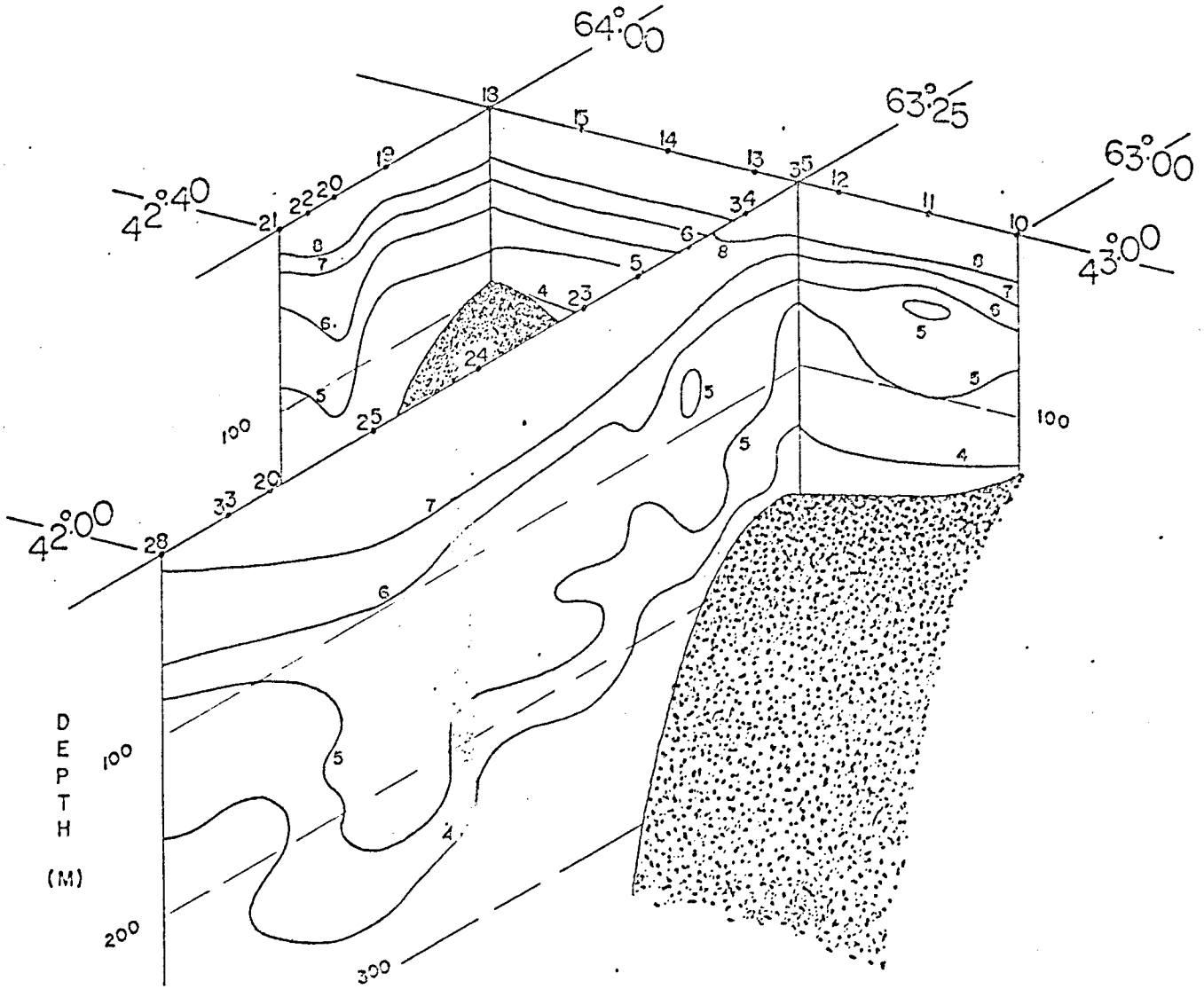

FIG 4(c)

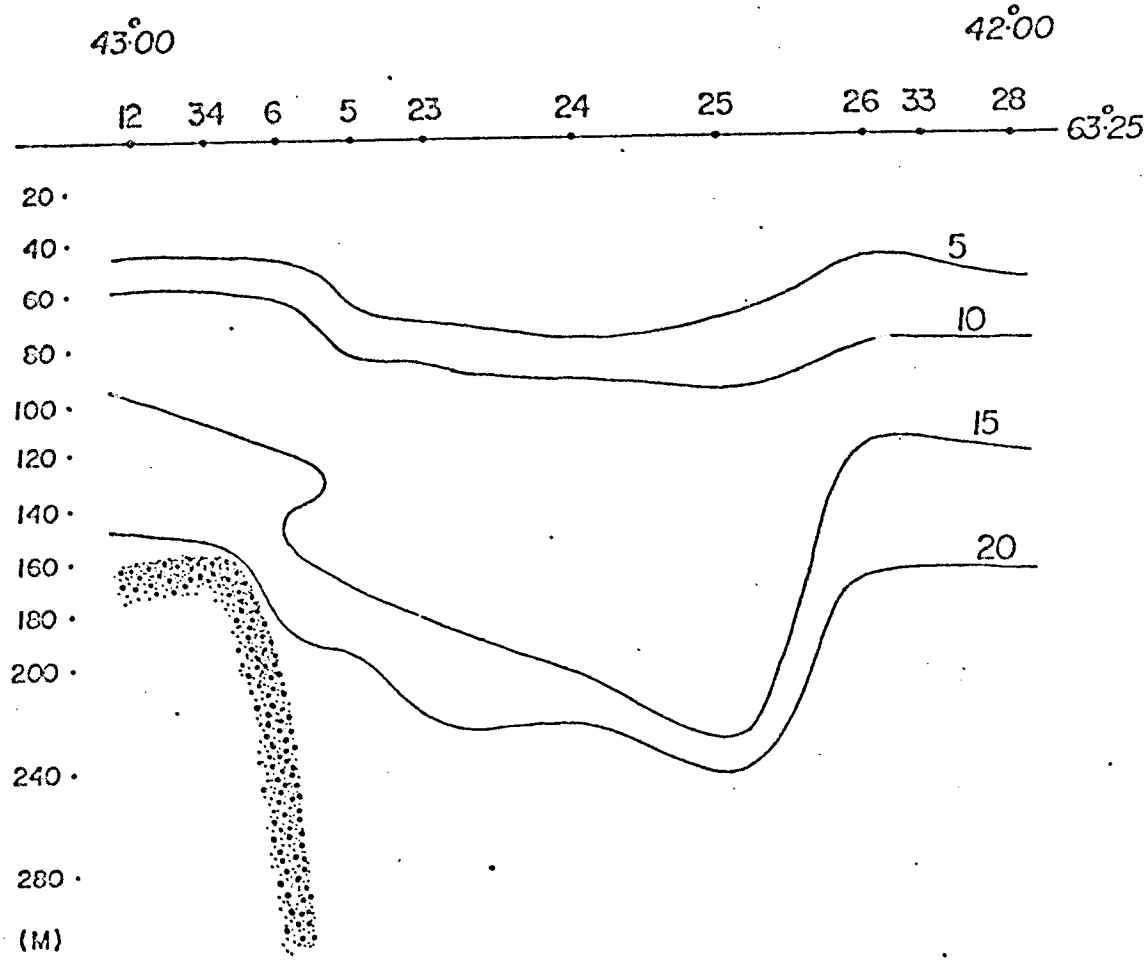
43°00
42°00
12
34
6
5
23
24
25
26
33
28
63°25
20
40
60
80
100
120
140
160
180
200
240
280
(M)
5
10
15
20

FIG 4(d)

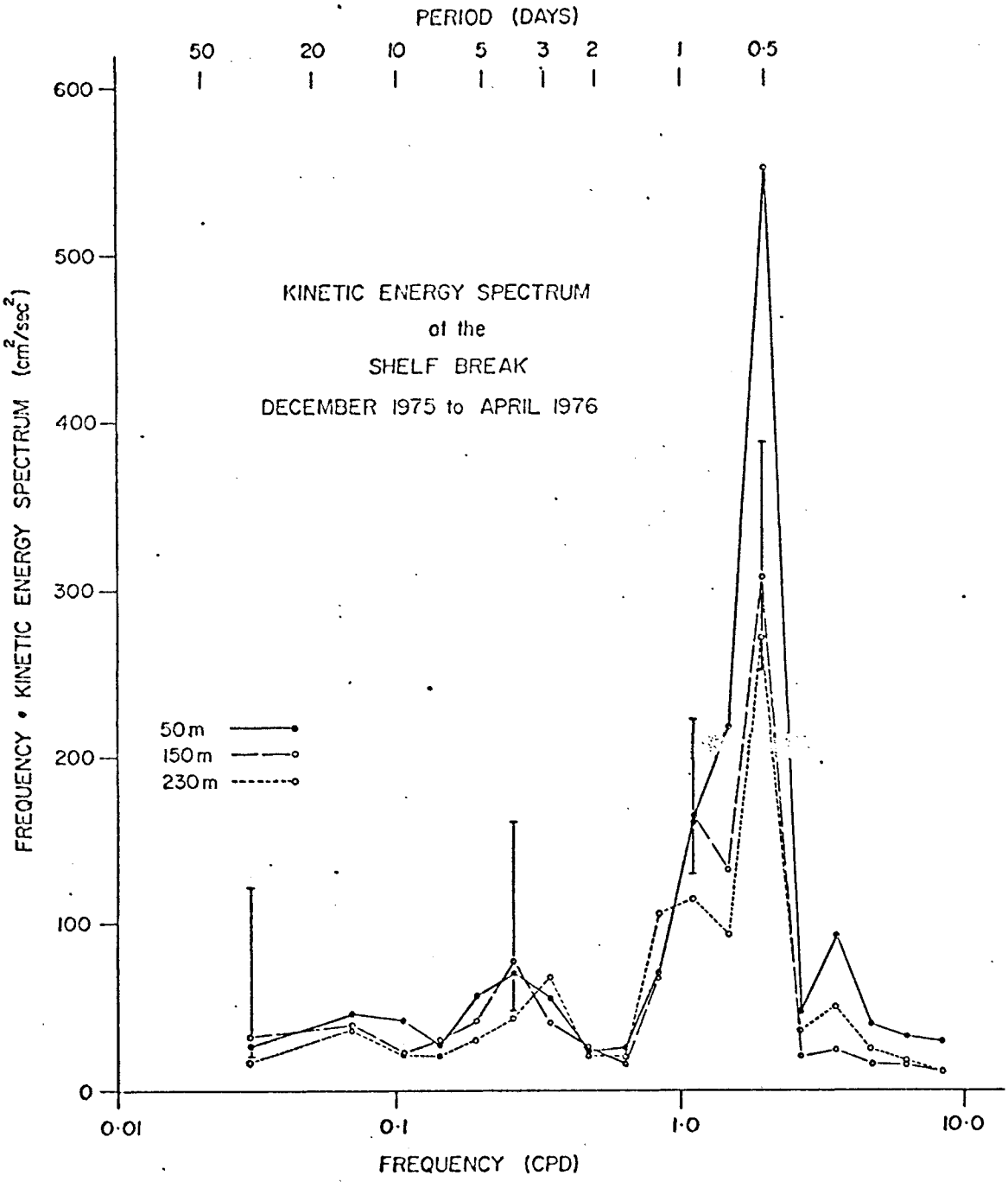
PERIOD (DAYS)
50
20
10
5
3
2
1
0·5
600
500
400
300
200
100
0
KINETIC ENERGY SPECTRUM
of the
SHELF BREAK
DECEMBER 1975 to APRIL 1976
FREQUENCY • KINETIC ENERGY SPECTRUM (cm²/sec²)
50m
150m
230m
0·01
0·1
1·0
10·0
FREQUENCY (CPD)

FIG 5

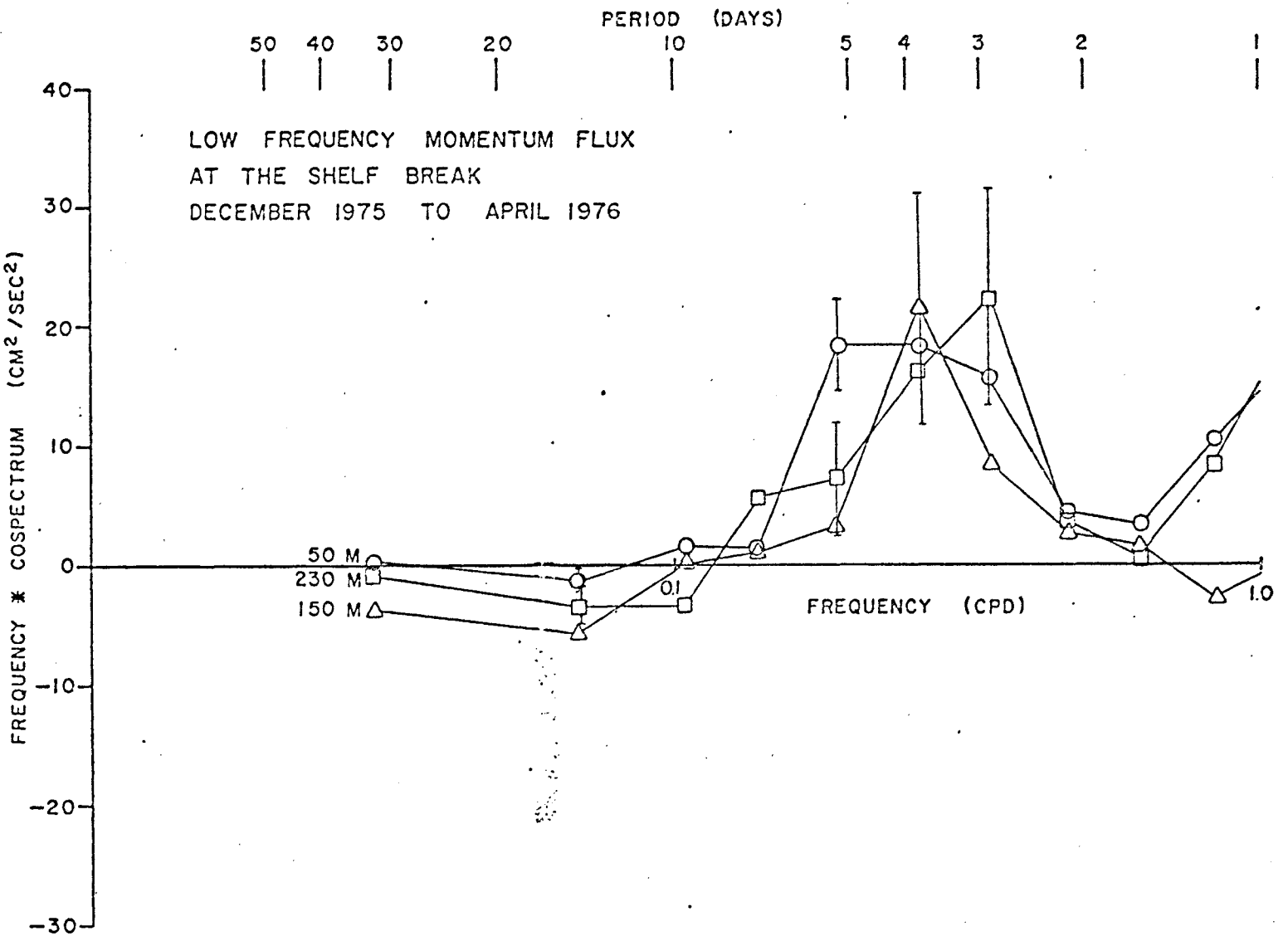
PERIOD (DAYS)
50 40 30 20 10 5 4 3 2 1
LOW FREQUENCY MOMENTUM FLUX
AT THE SHELF BREAK
DECEMBER 1975 TO APRIL 1976
FREQUENCY * COSPECTRUM (CM²/SEC²)
40
30
20
10
0
-10
-20
-30
50 M
230 M
150 M
0.1
1.0
FREQUENCY (CPD)

Fig 6

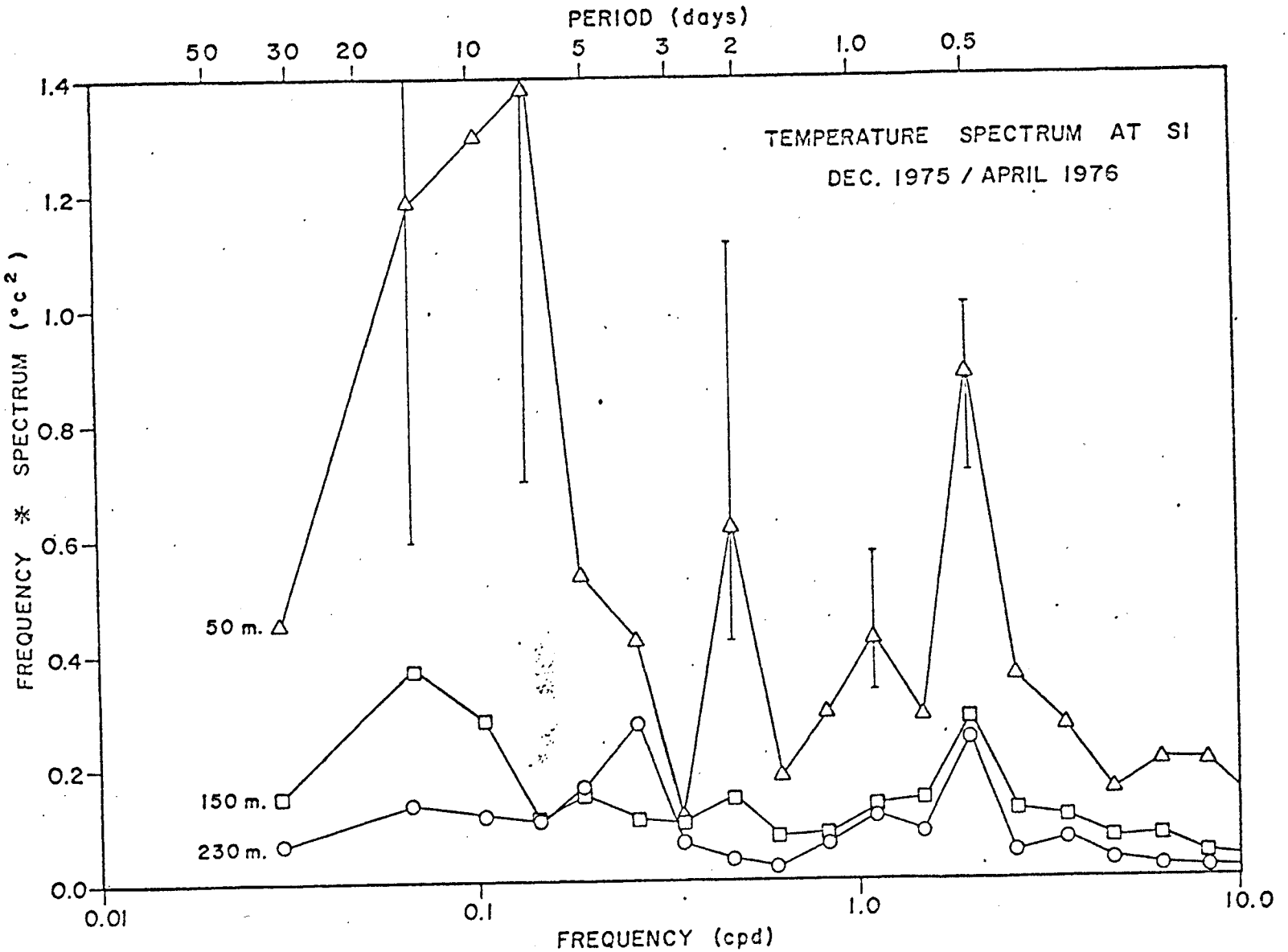
PERIOD (days)
50
30
20
10
5
3
2
1.0
0.5
TEMPERATURE SPECTRUM AT SI
DEC. 1975 / APRIL 1976
FREQUENCY * SPECTRUM (°c²)
1.4
1.2
1.0
0.8
0.6
0.4
0.2
0.0
50 m.
150 m.
230 m.
0.01
0.1
1.0
10.0
FREQUENCY (cpd)

FIG 7

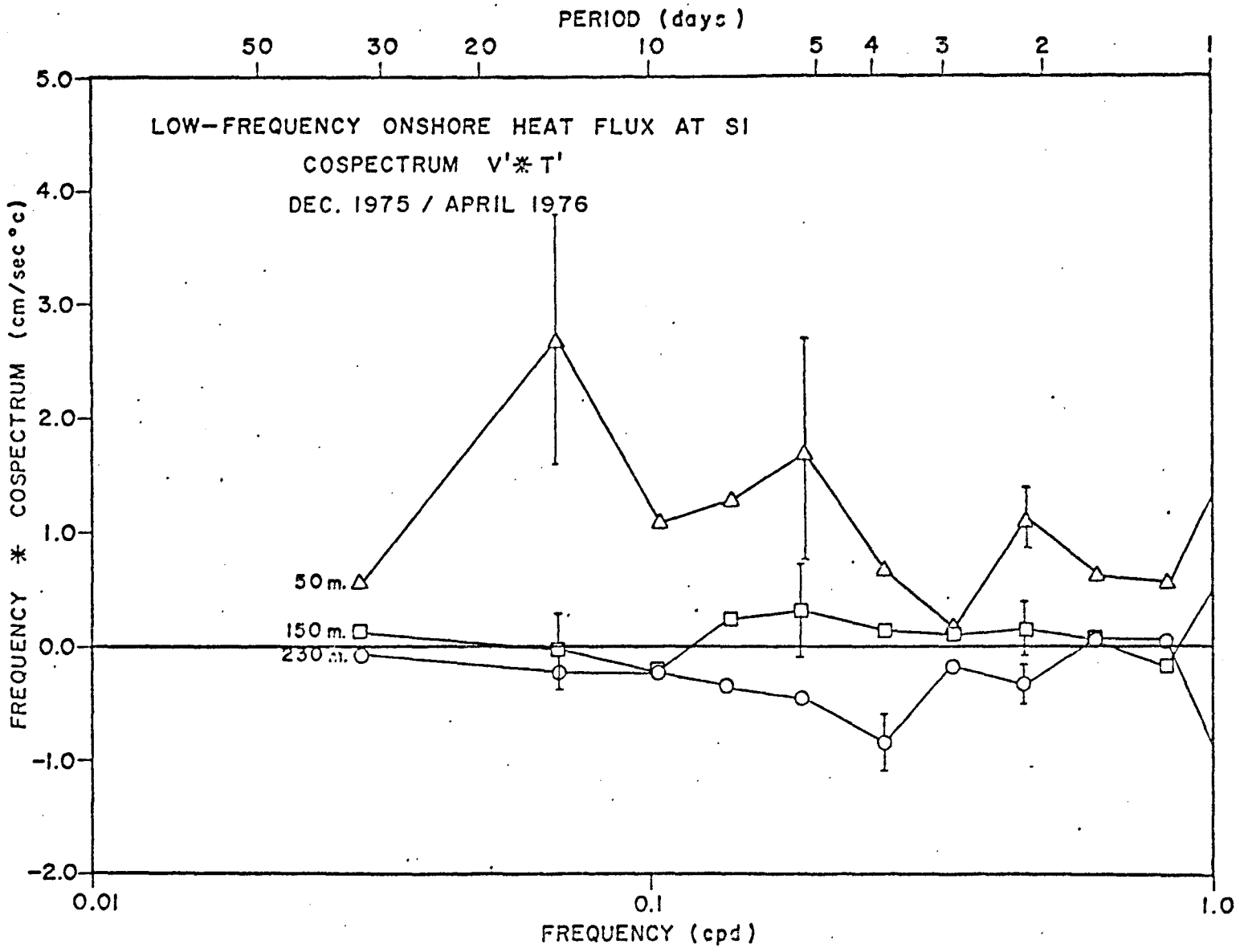
PERIOD (days)
50
30
20
10
5
4
3
2
1
LOW-FREQUENCY ONSHORE HEAT FLUX AT SI
COSPECTRUM V'* T'
DEC. 1975 / APRIL 1976
FREQUENCY * COSPECTRUM (cm/sec °c)
5.0
4.0
3.0
2.0
1.0
0.0
-1.0
-2.0
50 m.
150 m.
230 m.
0.01
0.1
1.0
FREQUENCY (cpd)

FIG 8(a)

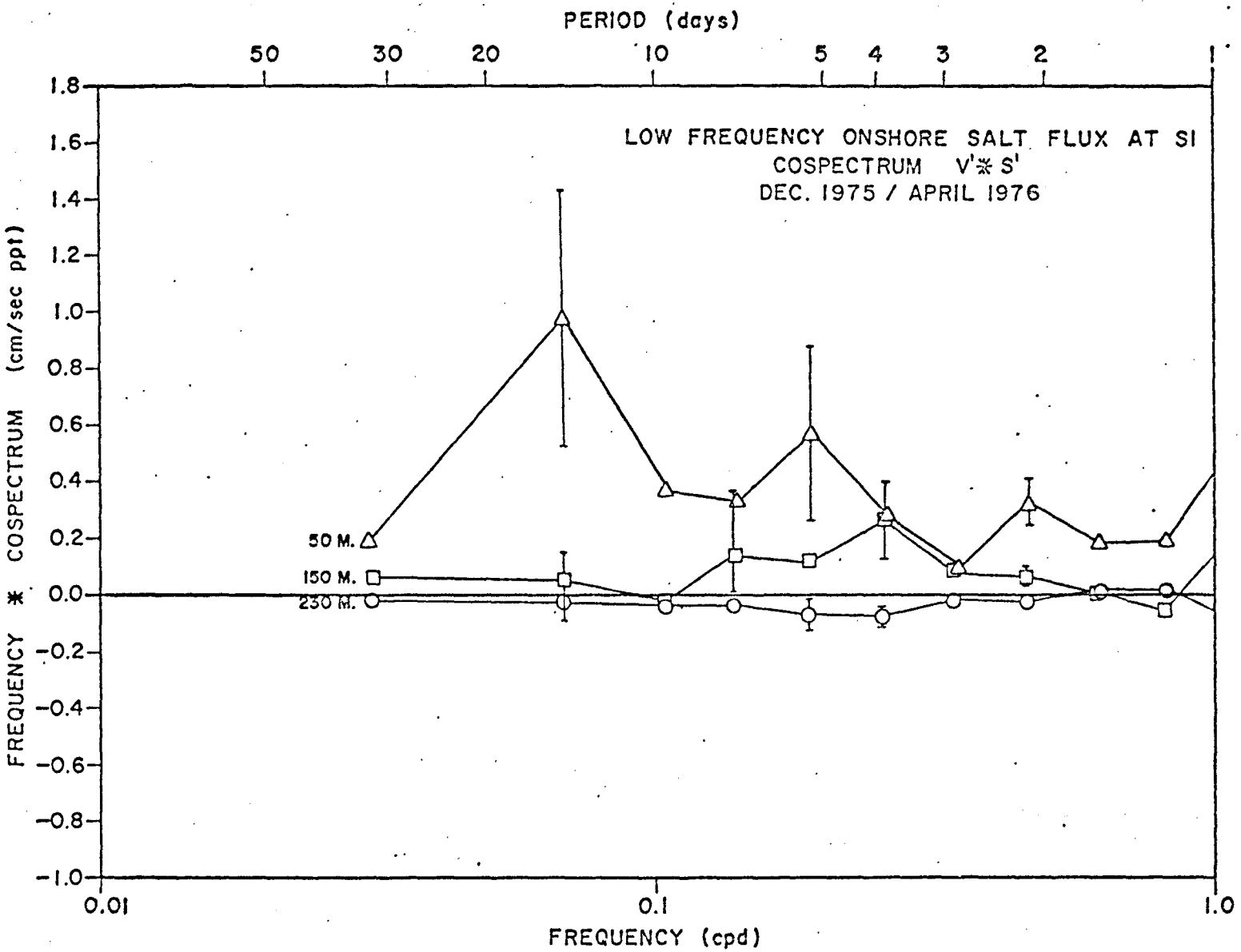
PERIOD (days)
50
30
20
10
5
4
3
2
1
LOW FREQUENCY ONSHORE SALT FLUX AT SI
COSPECTRUM V'* S'
DEC. 1975 / APRIL 1976
FREQUENCY * COSPECTRUM (cm/sec ppt)
1.8
1.6
1.4
1.2
1.0
0.8
0.6
0.4
0.2
0.0
-0.2
-0.4
-0.6
-0.8
-1.0
50 M.
150 M.
230 M.
0.01
0.1
1.0
FREQUENCY (cpd)

Fig 8(b)

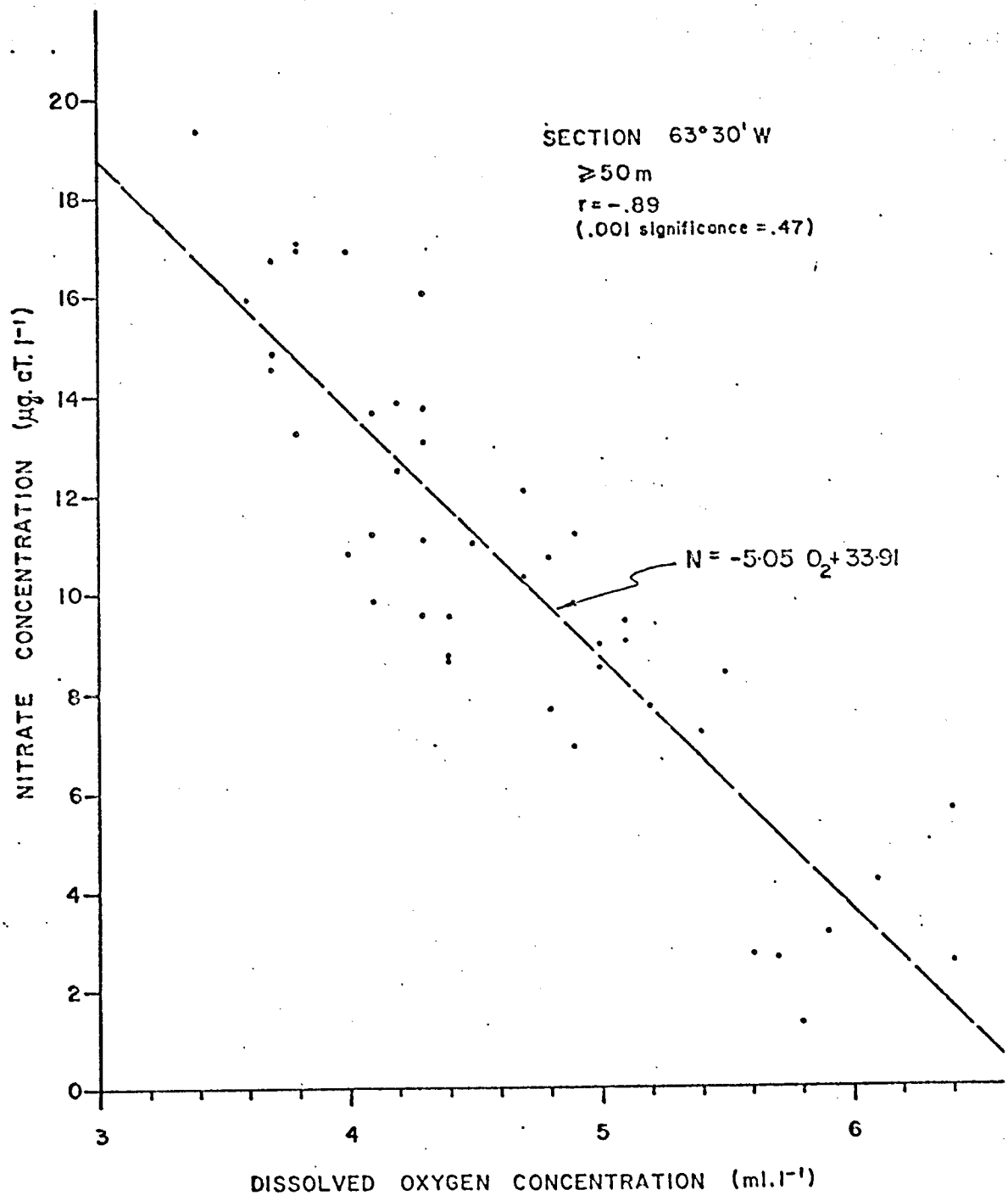
SECTION 63°30'W
≥50 m
r = -.89
(.001 significance = .47)
N = -5·05 O2 + 33·91
NITRATE CONCENTRATION (µg.gT. l-1)
DISSOLVED OXYGEN CONCENTRATION (ml.l-1)
0
2
4
6
8
10
12
14
16
18
20
3
4
5
6

FIG 9

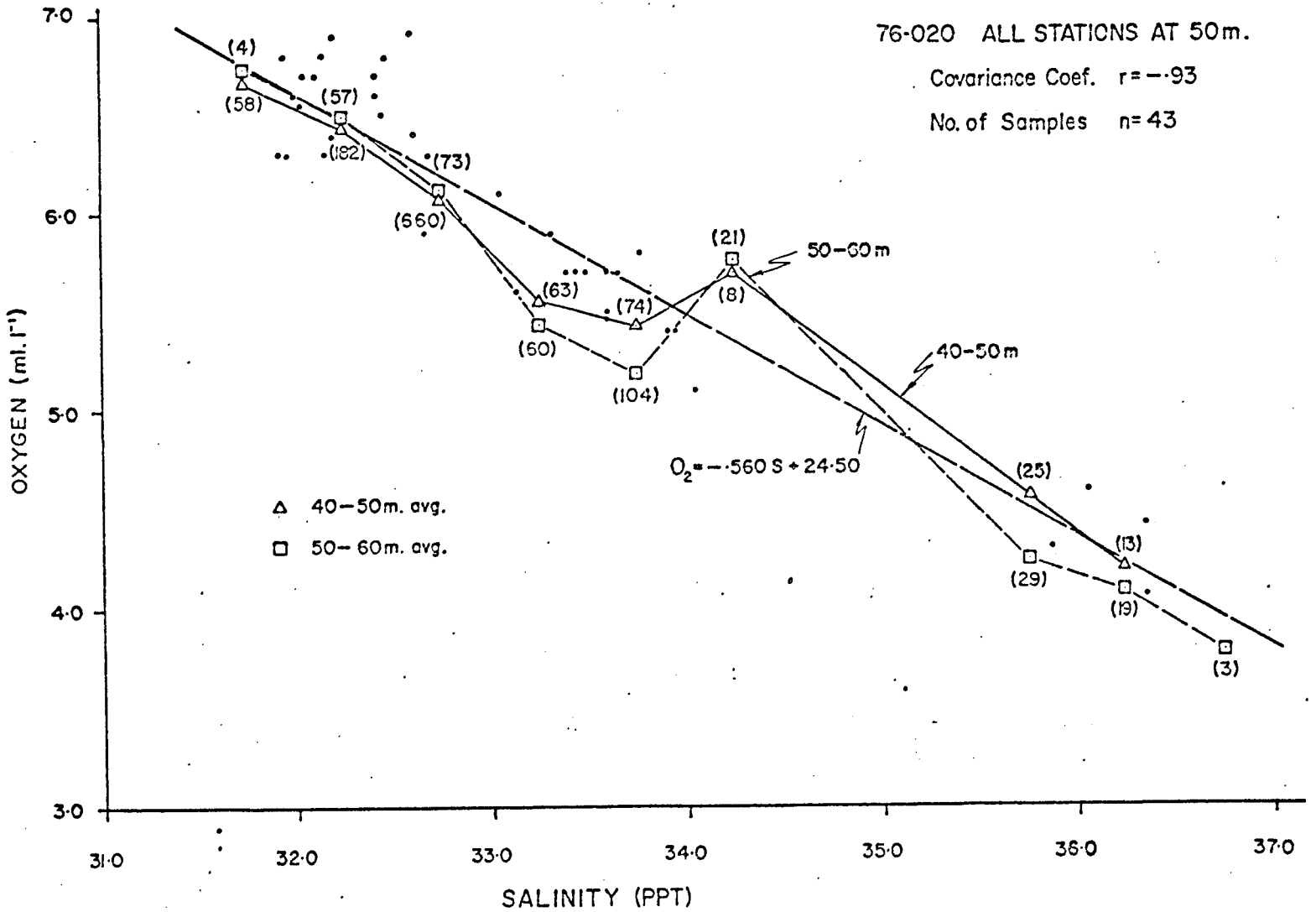
76-020 ALL STATIONS AT 50m.
Covariance Coef. r=-·93
No. of Samples n=43
(4)
(58)
(57)
(182)
(73)
(660)
(21)
50-60m
(8)
(63)
(74)
(60)
(104)
40-50m
O_2=-·560 S + 24·50
(25)
(13)
(29)
(19)
(3)
△ 40-50m. avg.
□ 50-60m. avg.
7·0
6·0
5·0
4·0
3·0
OXYGEN (ml.l⁻¹)
31·0
32·0
33·0
34·0
35·0
36·0
37·0
SALINITY (PPT)

FIG 10(a)

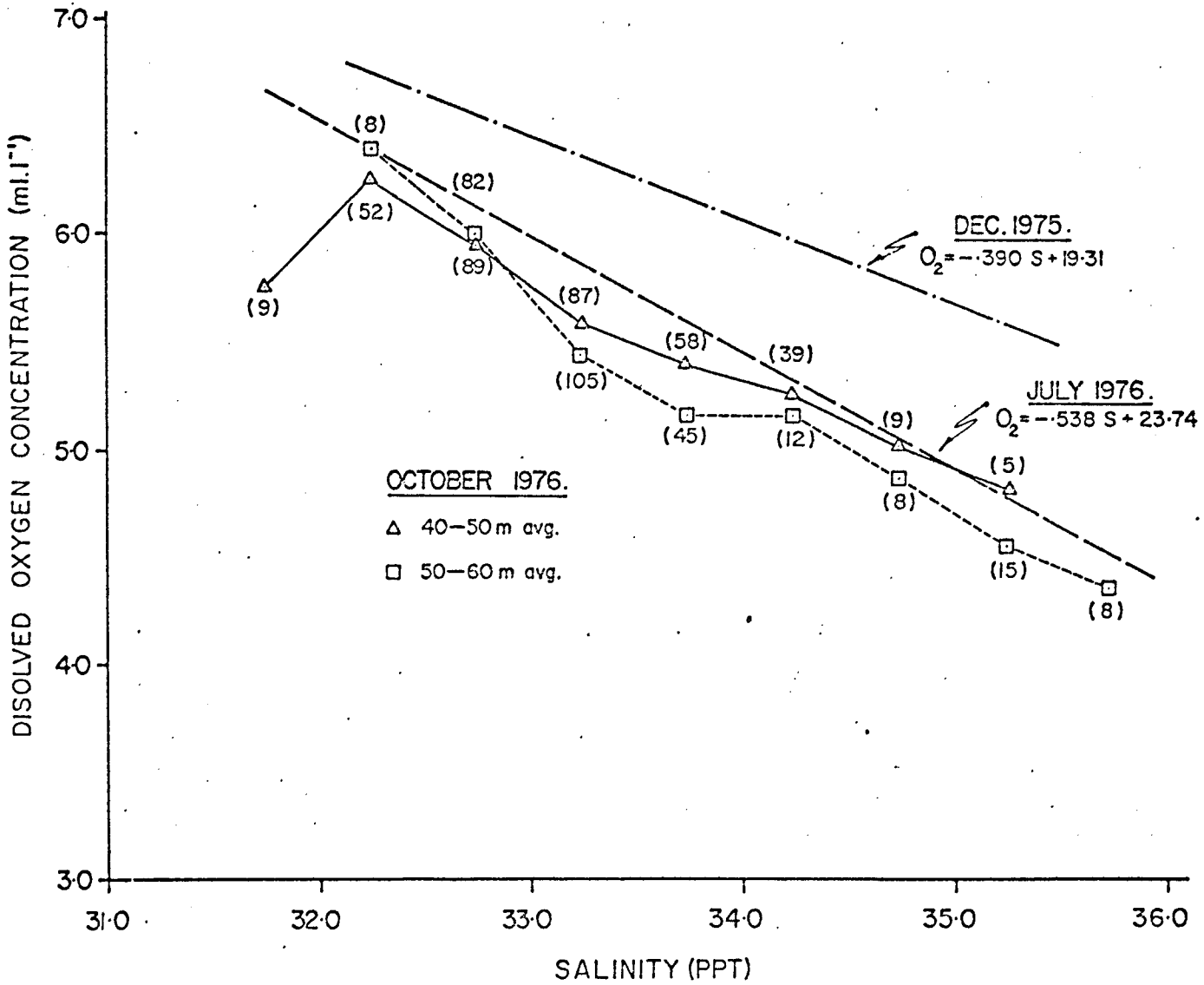
DISOLVED OXYGEN CONCENTRATION (ml.l⁻¹)
7·0
6·0
5·0
4·0
3·0
31·0
32·0
33·0
34·0
35·0
36·0
SALINITY (PPT)
DEC. 1975.
O2 = −·390 S + 19·31
JULY 1976.
O2 = −·538 S + 23·74
OCTOBER 1976.
△ 40–50 m avg.
□ 50–60 m avg.
(8)
(82)
(52)
(89)
(9)
(87)
(58)
(39)
(105)
(9)
(45)
(12)
(5)
(8)
(15)
(8)

Fig 10(b)

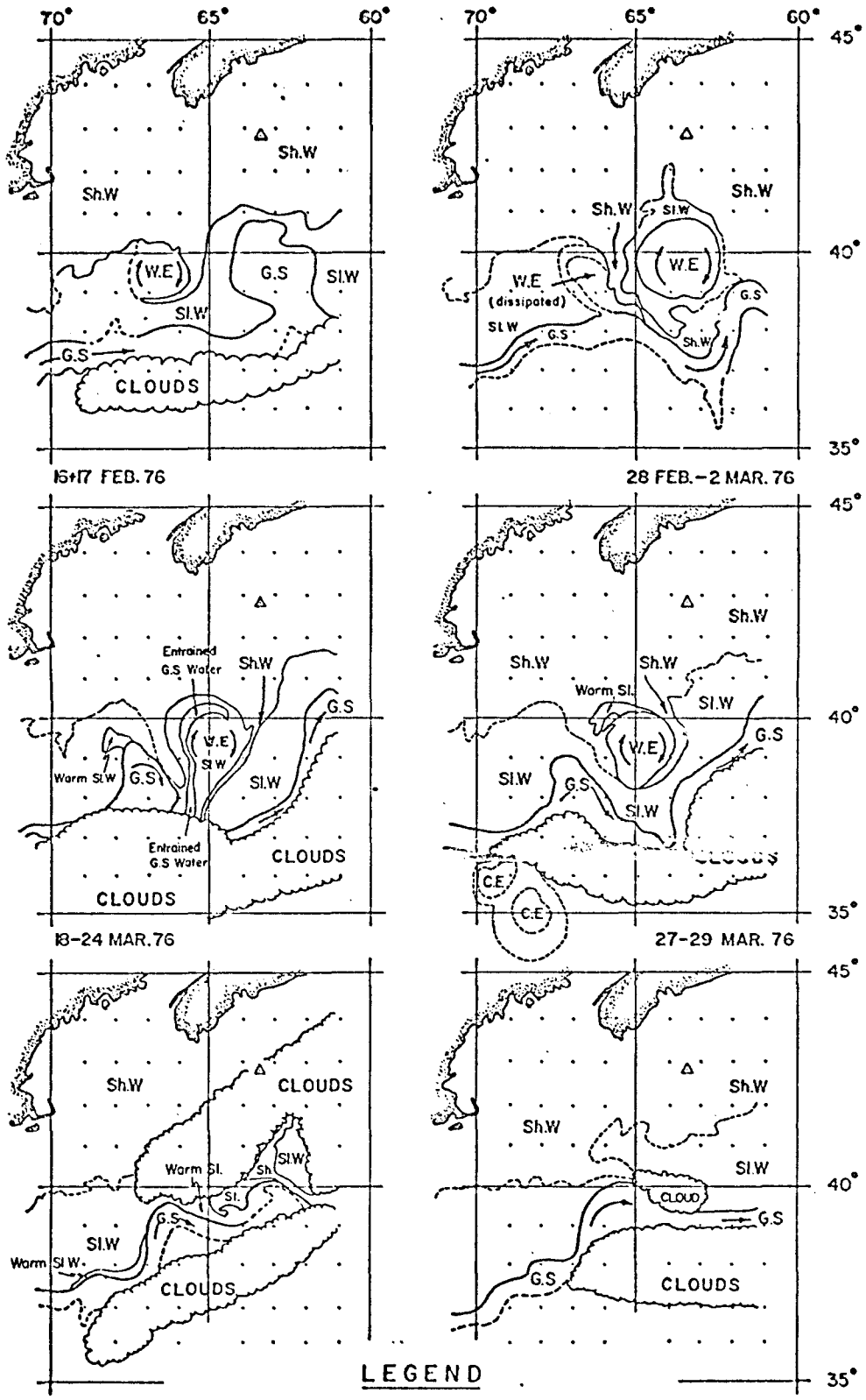
70°
65°
60°
45°
40°
35°
Sh.W
W.E
G.S
Sl.W
CLOUDS
16+17 FEB. 76
W.E (dissipated)
28 FEB.–2 MAR. 76
Entrained G.S Water
Warm Sl.W
Warm Sl.
13–24 MAR. 76
C.E
27–29 MAR. 76
Sl.
Sh
CLOUD
3–7 APR. 76
11–14 APR. 76
LEGEND
G.S. GULF STREAM
Sh.W SHELF WATER
Sl.W. SLOPE WATER
C.E. COLD EDDY
W.E. WARM EDDY
MOORING

Fig 11

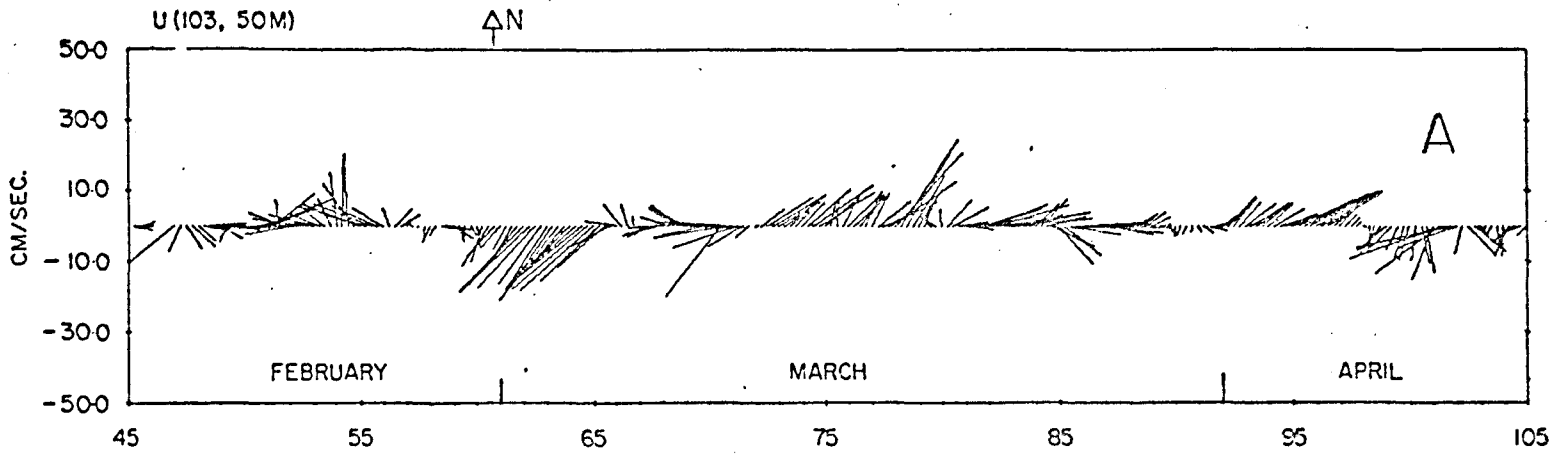

42°48'38 N. • INST. NO. 1286 • STARTING 05:26 HRS • DAY 45 1976.

63°30'27 W. • DEPTH 50 M • STATION 103 • CRUISE 75-033

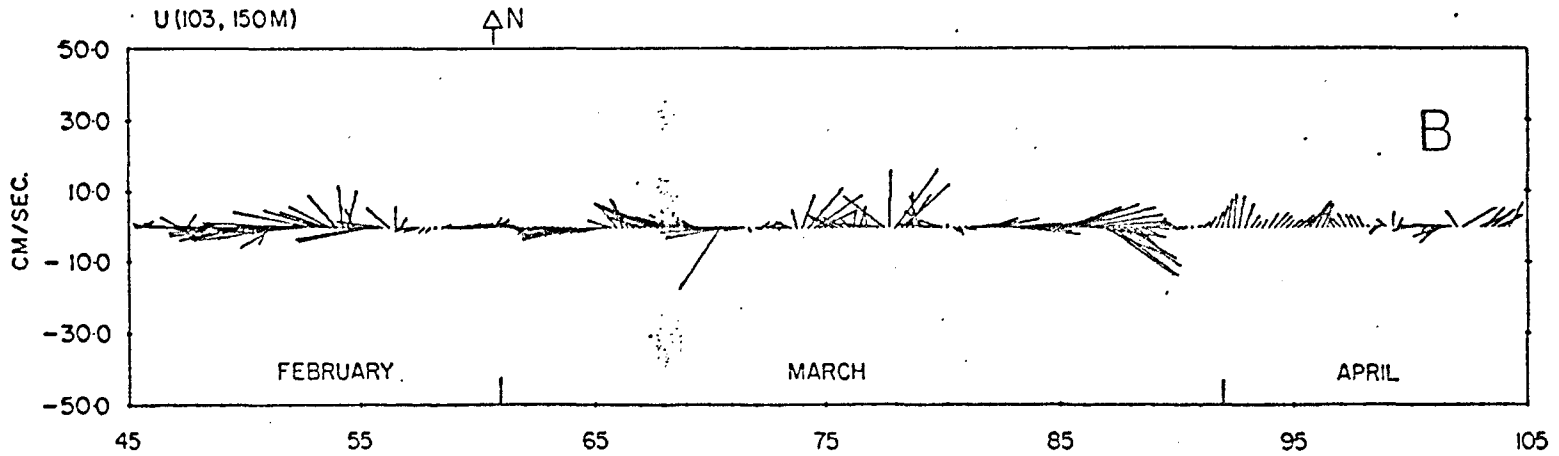

42°48'38 N. • INST. NO. 1287 • STARTING 05:42 HRS • DAY 45 1976.

63°30'27 W. • DEPTH 150 M • STATION 103 • CRUISE 75-033

FIG 12(a).

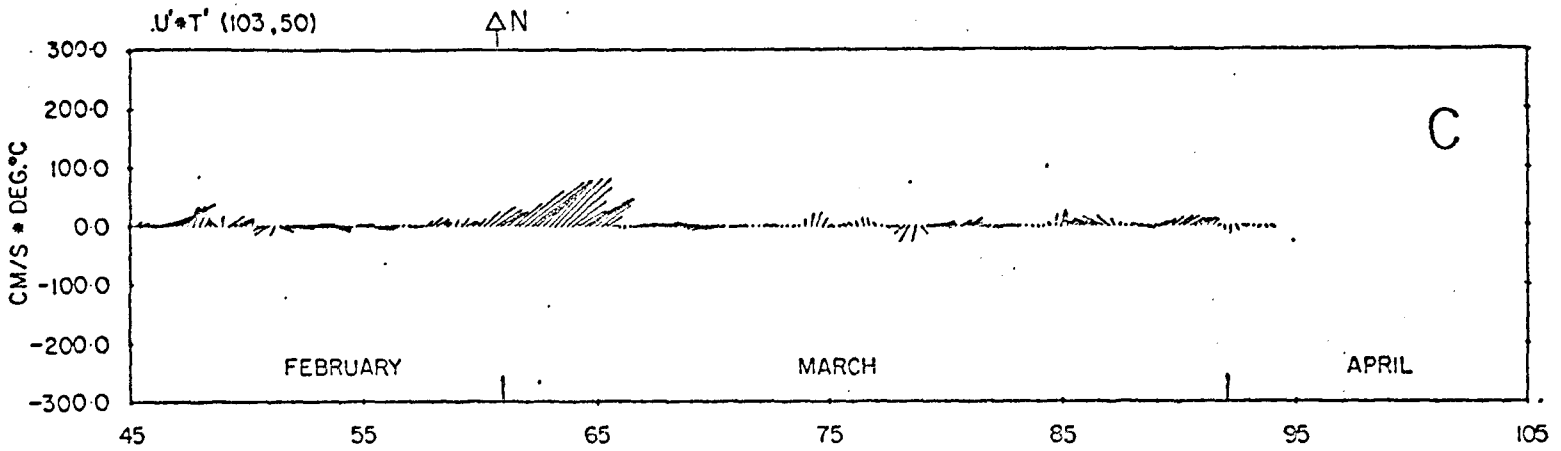

42°48'38 N. • INST. NO. 1286 • STARTING 05·26 HRS. • DAY 45 1976.

63°30'27 W. • DEPTH 50 M • STATION 103 • CRUISE 75-033.

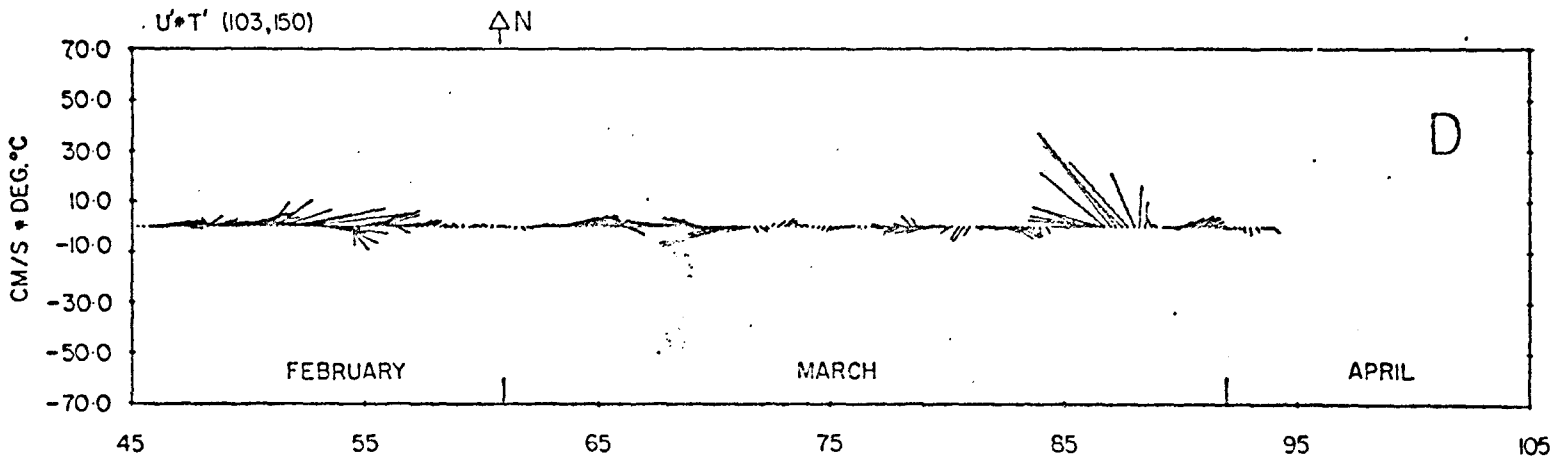

42°48'38 N. • INST. NO. 1287 • STARTING 05·42 HRS • DAY 45 1976.

63°30'27 W. • DEPTH 150 M • STATION 103 • CRUISE 75-033

Fig 12 (b)

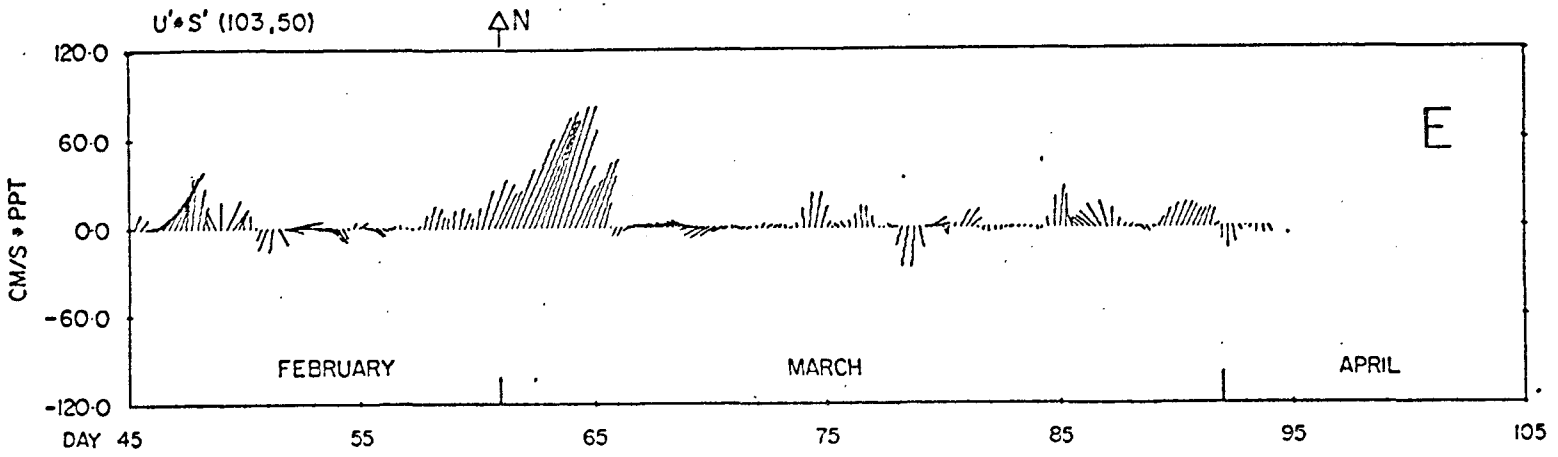

42°48'38 N. • INST. NO. 1286 • STARTING 05·26 HRS. • DAY 45 1976

63°30'27 W. • DEPTH 50 M • STATION 103 • CRUISE 75-033

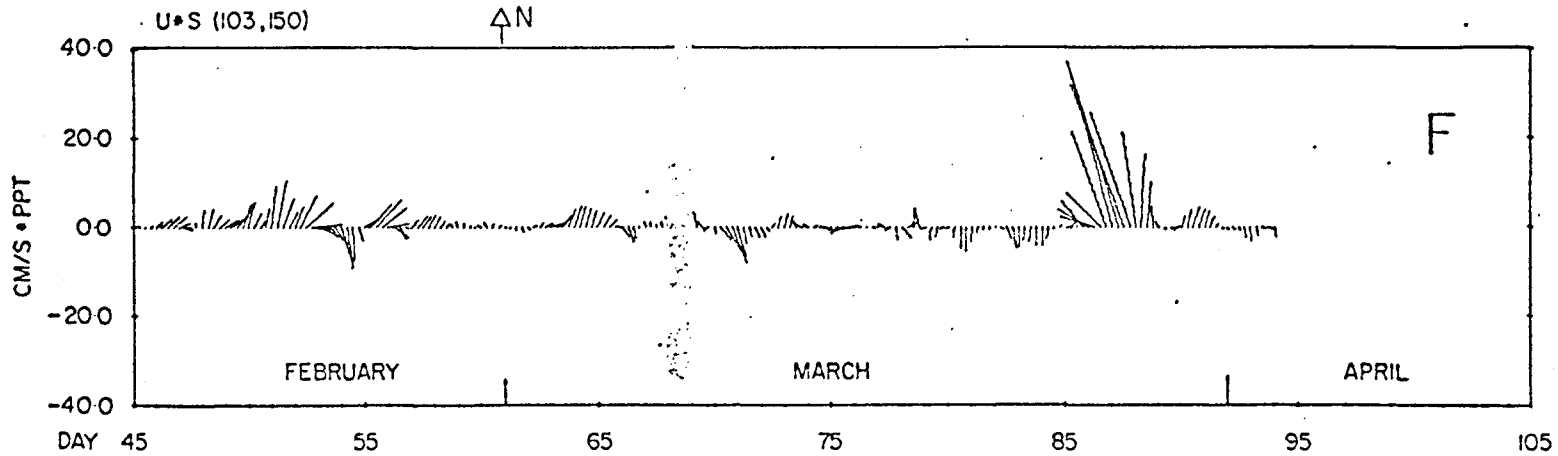

42°48'38 N. • INST. NO. 1287 • STARTING 05·42 HRS • DAY 45 1976.

63°30'27 W. • DEPTH 150 M • STATION 103 • CRUISE 75-033

FIG 12 (c)

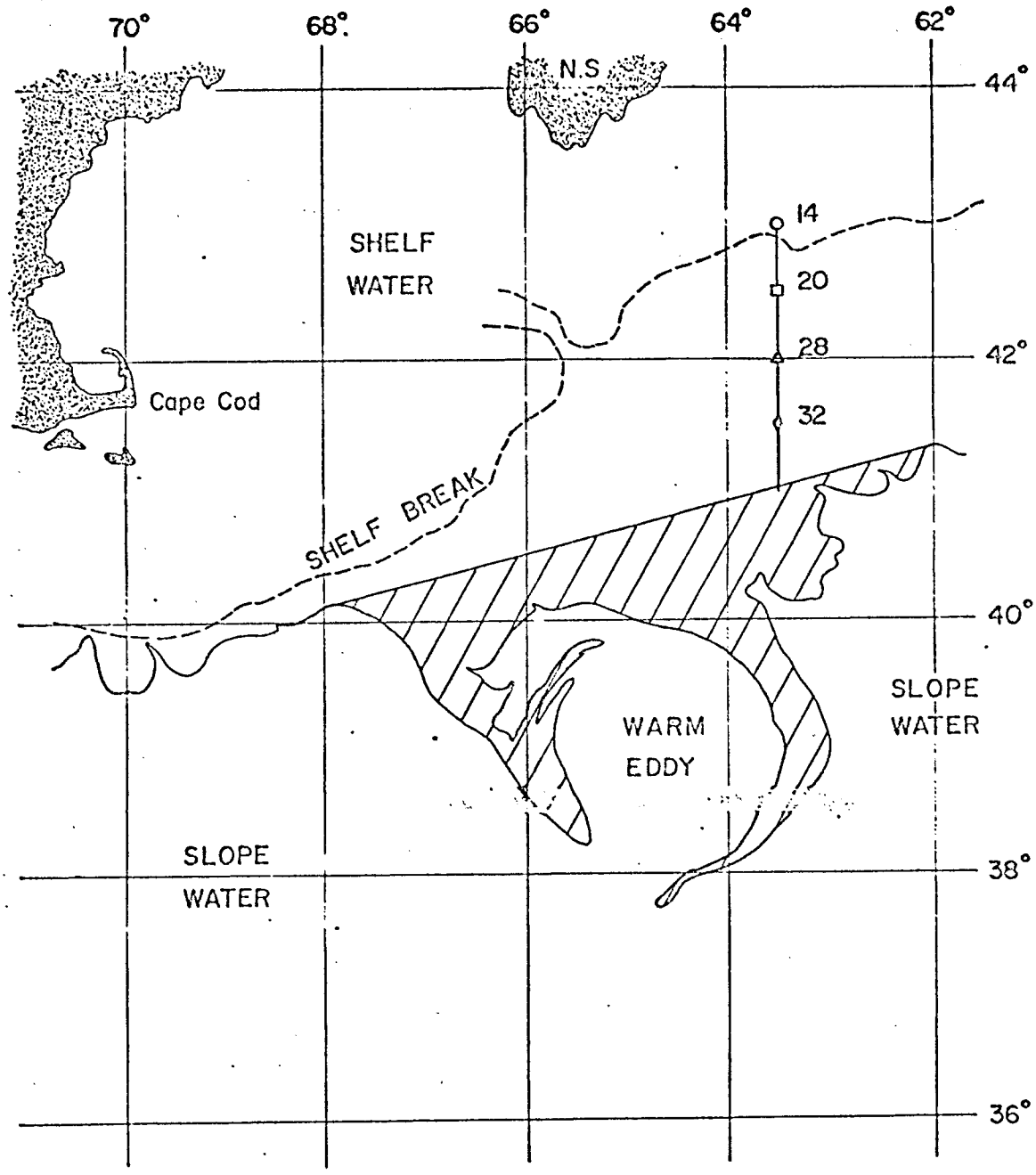
70°
68°
66°
64°
62°
44°
42°
40°
38°
36°
N.S
SHELF
WATER
14
20
28
32
Cape Cod
SHELF BREAK
WARM
EDDY
SLOPE
WATER
SLOPE
WATER

FIG 13(a)

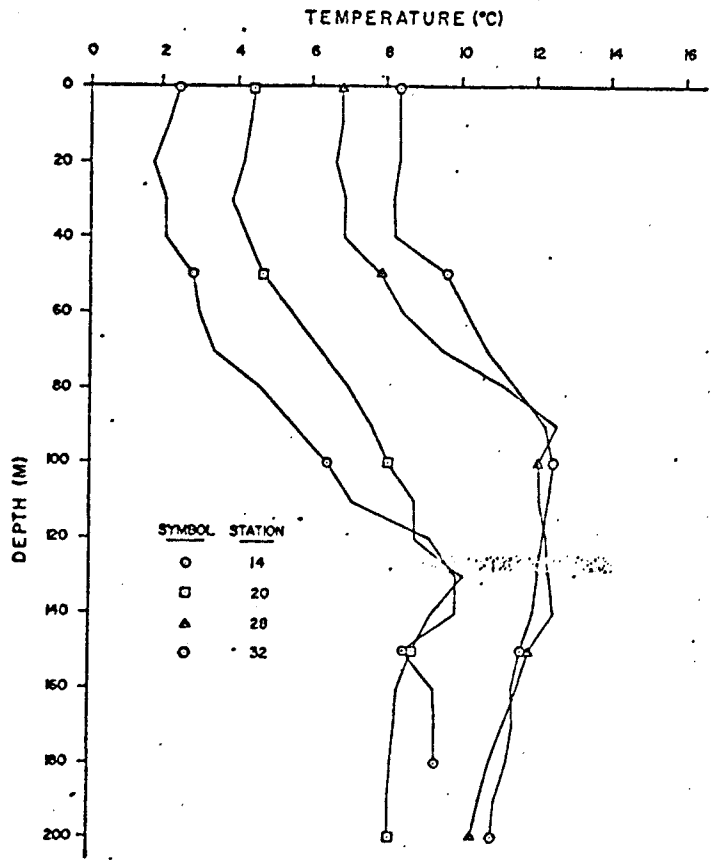
TEMPERATURE (°C)
0
2
4
6
8
10
12
14
16
DEPTH (M)
0
20
40
60
80
100
120
140
160
180
200
SYMBOL
STATION
14
20
28
32

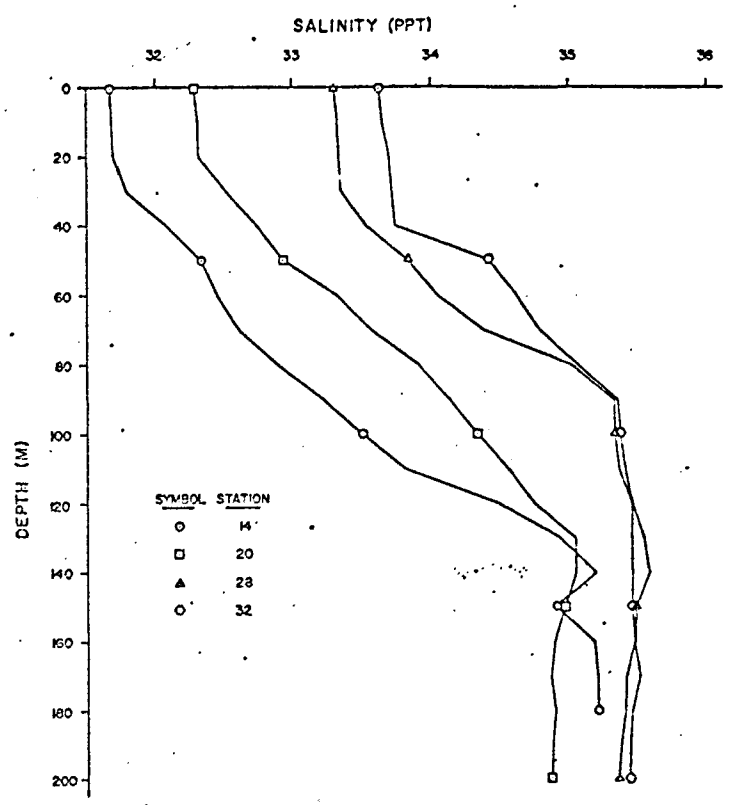
SALINITY (PPT)
32
33
34
35
36
DEPTH (M)
0
20
40
60
80
100
120
140
160
180
200
SYMBOL
STATION
14
20
28
32

FIG 13 (b)